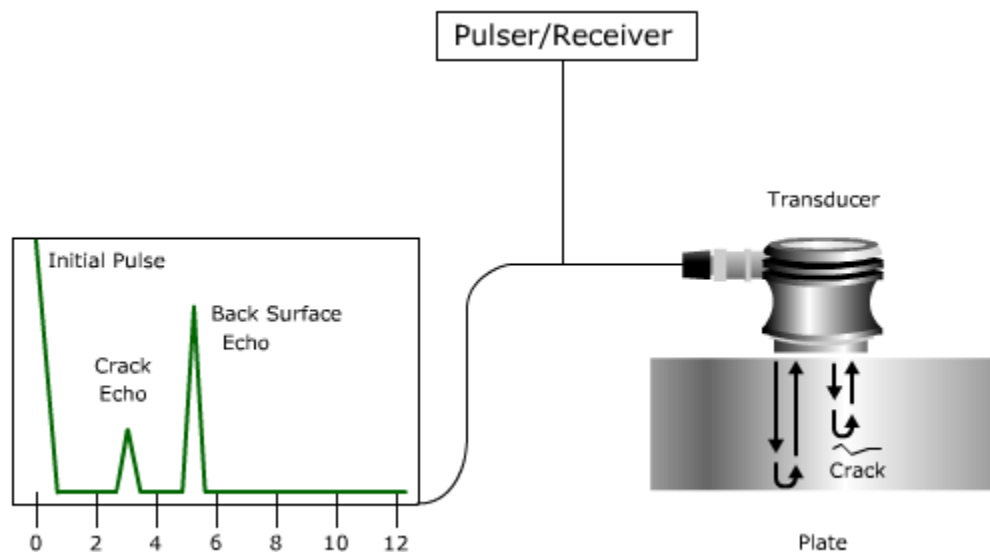


## Basic Principles of Ultrasonic Testing

Ultrasonic Testing (UT) uses high frequency sound energy to conduct examinations and make measurements. Ultrasonic inspection can be used for flaw detection/evaluation, dimensional measurements, material characterization, and more. To illustrate the general inspection principle, a typical pulse/echo inspection configuration as illustrated below will be used.

A typical UT inspection system consists of several functional units, such as the pulser/receiver, transducer, and display devices. A pulser/receiver is an electronic device that can produce high voltage electrical pulse. Driven by the pulser, the transducer generates high frequency ultrasonic energy. The sound energy is introduced and propagates through the materials in the form of waves. When there is a discontinuity (such as a crack) in the wave path, part of the energy will be reflected back from the flaw surface. The reflected wave signal is transformed into electrical signal by the transducer and is displayed on a screen. In the applet below, the reflected signal strength is displayed versus the time from signal generation to when an echo was received. Signal travel time can be directly related to the distance that the signal traveled. From the signal, information about the reflector location, size, orientation and other features can sometimes be gained.



## History of Ultrasonics

Prior to World War II, [sonar](#), the technique of sending sound waves through water and observing the returning echoes to characterize submerged objects, inspired early ultrasound investigators to explore ways to apply the concept to medical diagnosis. In 1929 and 1935, Sokolov studied the use of ultrasonic waves in detecting metal objects. Mulhauser, in 1931, obtained a patent for using ultrasonic waves, using two [transducers](#) to detect flaws in solids. Firestone (1940) and Simons (1945) developed pulsed ultrasonic testing using a pulse-echo technique.

Shortly after the close of World War II, researchers in Japan began to explore medical diagnostic capabilities of ultrasound. The first ultrasonic instruments used an A-mode presentation with blips on an [oscilloscope](#) screen. That was followed by a B-mode presentation with a two dimensional, gray scale imaging.

Japan's work in ultrasound was relatively unknown in the United States and Europe until the 1950s. Then researchers presented their findings on the use of ultrasound to detect gallstones, breast masses, and tumors to the international medical community. Japan was also the first country to apply Doppler ultrasound, an application of ultrasound that detects internal moving objects such as blood coursing through the heart for cardiovascular investigation.

Ultrasound pioneers working in the United States contributed many innovations and important discoveries to the field during the following decades. Researchers learned to use ultrasound to detect potential cancer and to visualize tumors in living subjects and in excised tissue. Real-time imaging, another significant diagnostic tool for physicians, presented ultrasound images directly on the system's CRT screen at the time of scanning. The introduction of spectral Doppler and later color Doppler depicted blood flow in various colors to indicate speed of flow and direction.



The United States also produced the earliest hand held "contact" scanner for clinical use, the second generation of B-mode equipment, and the prototype for the first articulated-arm hand held scanner, with 2-D images.

## Beginnings of Nondestructive Evaluation (NDE)

Nondestructive testing has been practiced for many decades, with initial rapid developments in instrumentation spurred by the technological advances that occurred during World War II and the subsequent defense effort. During the earlier days, the primary purpose was the detection of defects. As a part of "safe life" design, it was intended that a structure should not develop macroscopic defects during its life, with the detection of such defects being a cause for removal of the component from service. In response to this need, increasingly sophisticated techniques using ultrasonics, eddy currents, x-rays, dye penetrants, magnetic particles, and other forms of interrogating energy emerged.

In the early 1970's, two events occurred which caused a major change. The continued improvement of the technology, in particular its ability to detect small flaws, led to the unsatisfactory situation that more and more parts had to be rejected, even though the probability of failure had not changed. However, the discipline of fracture mechanics emerged, which enabled one to predict whether a crack of a given size would fail under a particular load if a material property, fracture toughness, were known. Other laws were developed to predict the rate of growth of cracks under cyclic loading (fatigue). With the advent of these tools, it became possible to accept structures containing defects if the sizes of those defects were known. This formed the basis for new philosophy of "fail safe" or "damage tolerant" design. Components having known defects could continue in service as long as it could be established that those defects would not grow to a critical, failure producing size.

A new challenge was thus presented to the nondestructive testing community. Detection was not enough. One needed to also obtain quantitative information about flaw size to serve as an input to fracture mechanics based predictions of remaining life. These concerns, which were felt particularly strongly in the defense and nuclear power industries, led to the creation of a number of research programs around the world and the emergence of quantitative nondestructive evaluation (QNDE) as a new discipline. The Center for Nondestructive Evaluation at Iowa State University (growing out of a major research effort at the Rockwell International Science Center); the Electric Power Research Institute in Charlotte, North Carolina; the Fraunhofer Institute for Nondestructive Testing in Saarbrücken, Germany; and the Nondestructive Testing Centre in Harwell, England can all trace their roots to those.

## Present State of Ultrasonics

Ultrasonic testing (UT) has been practiced for many decades now. Initial rapid developments in instrumentation spurred by the technological advances from the 1950's continue today. Through the 1980's and continuing into the present computers have provided technicians with smaller and more rugged instruments with greater capabilities.



Thickness gauging is one example of instruments that have been refined to reduce operator error and time on task by recording readings. This reduces the need for a "scribe" and allows the technician to record as many as 54,000 thickness values before downloading to a computer. Some instruments have the capability to capture waveforms as well as thickness readings. The waveform option allows a technician to view or review the A-scan signal of thickness readings without being present during the inspection. Much research and development has gone into the understanding of sound reflected from a surfaces that contains pitting or erosion as would be found on the inner surface of a pipe carrying product. This has lead to more consistent and accurate field measurements.

For sometime ultrasonic flaw detectors have incorporated a trigonometric function allowing for fast and accurate location of indications when performing shear wave inspections. Cathode ray tubes, for the most part, have been replaced with LED or LCD screens. These screens in most cases are extremely easy to view in a wide range of ambient lighting. Bright or low light working conditions encountered by technicians have little effect on the technician's ability to view the screen. Screens can be adjusted for brightness, contrast, and on some instruments even the color of the screen and signal can be selected. Transducers can be programed with predetermined instrument settings. The technician only has to place the transducer in contact with the instrument, the instrument will then set variables such as range, delay, frequency, and gain as it is directed by the "chip" in the transducer.

Along with computers, robotics have contributed to the advancement of ultrasonic inspections. Early on the advantage of a stationary platform was recognized and used in industry. These systems were produced by a number of companies. Automated systems produced a system known as the Ultragraph 1020A. This system consisted of an immersion tank, bridge, and recording system for a printout of the scan. The resultant C-scan provides a plan or top view of the component. Scanning of components was considerably faster than contact hand scanning, and the system provided a record of the inspection. Limitations included size and shape of the component, and also system cost.

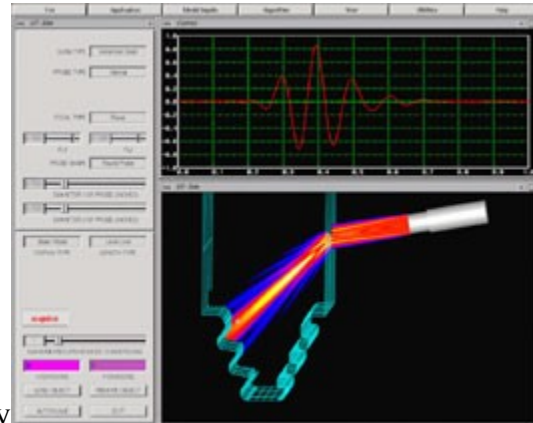
Immersion systems have advanced in many directions since the the 1960's. While robotics, as we know it, did not exist, the "immersion tanks" provided effective and sired inquiry into other means of inspection. Today robotics have allowed immersion transducers to inspect components without the need for immersing them in water. Squirter systems allow the transducer to pass over the component transmitting sound through a water column. Computers can be programed to inspect large, complex shaped components, with one or multiple transducers collecting information. This information is then collected by a computer for evaluation, transmission to a customer, and finally archival of an image that will maintain quality for years to come.



Today quantitative theories have been developed to describe the interaction of the interrogating fields with flaws. Models incorporating the results have been integrated with solid model descriptions of real-part geometry's to simulate practical inspections. Related tools allow NDE to be considered during the design process on an equal footing with other failure-related engineering disciplines. Quantitative descriptions of NDE performance, such as the probability of detection (POD), have become an integral part of statistical risk assessment. Measurement procedures initially developed for metals have been extended to engineered materials such as composites, where anisotropy and inhomogeneity have become important issues. The rapid advances in digitization and computing capabilities have totally changed the faces of many instruments and the type of algorithms that are used in processing the resulting data. High-resolution imaging systems and multiple measurement modalities for characterizing a flaw have emerged. Interest is increasing not only in detecting, characterizing, and sizing defects, but in characterizing the materials in which they occur. Goals range from the determination of fundamental microstructural characteristics such as grain size, [porosity](#), and texture (preferred grain orientation), to material properties related to such failure mechanisms as fatigue, creep, and fracture toughness. As technology continues to advance, applications of ultrasound advances. The high-resolution imaging systems in the laboratory today will be tools of the technician tomorrow.

## Future Direction of Ultrasonic Inspection

Looking to the future, those in the field of NDE see an exciting new set of opportunities. Defense and nuclear power industries have played a major role in the emergence of NDE. Increasing global competition has led to dramatic changes in product development and business cycles. At the same time aging infrastructure, from roads to buildings and aircraft, present a new set of measurement and monitoring challenges for engineers as well as technicians.



Among the new applications of NDE spawned by these changes is the increased emphasis on the use of NDE to improve productivity of manufacturing processes. Quantitative nondestructive evaluation (QNDE) both increases the amount of information about failure modes and the speed with which information can be obtained and facilitates the development of in-line measurements for process control.

The phrase, "you can not inspect in quality, you must build it in," exemplifies the industry's focus on avoiding the formation of flaws. Nevertheless, flaws and the need to identify them, both during manufacture and in service, will never disappear and continual development of flaw detection and characterization techniques are necessary.

Advanced simulation tools that are designed for inspectability and their integration into quantitative strategies for life management will contribute to increase the number and types of engineering applications of NDE. With growth in engineering applications for NDE, there will be a need to expanded the knowledge base of technicians performing the evaluations. Advanced simulation tools used in the design for inspectability may be used to provide technical students with a greater understanding of sound behavior in materials. UTSIM developed at Iowa State University provides a glimpse into what may be used in the technical classroom as an interactive laboratory tool.

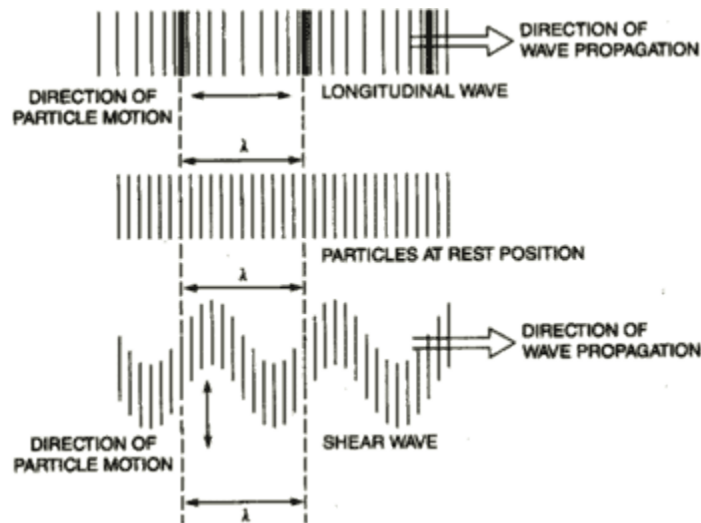
As globalization continues, companies will seek to develop, with ever increasing frequency, uniform international practices. In the area of NDE, this trend will drive the emphases on standards, enhanced educational offerings, and simulations that can be communicated electronically.

The coming years will be exciting as NDE will continue to emerge as a full-fledged engineering discipline.

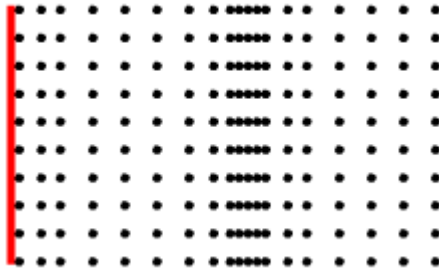
## Wave Propagation

Ultrasonic testing is based on time-varying deformations or vibrations in materials, which is generally referred to as acoustics. All material substances are comprised of atoms, which may be forced into [vibrational motion](#) about their equilibrium positions. Many different patterns of vibrational motion exist at the atomic level, however, most are irrelevant to acoustics and ultrasonic testing. Acoustics is focused on particles that contain many atoms that move in unison to produce a mechanical wave. When a material is not stressed in tension or compression beyond its elastic limit, its individual particles perform elastic oscillations. When the particles of a medium are displaced from their equilibrium positions, internal (electrostatic) restoration forces arise. It is these elastic restoring forces between particles, combined with inertia of the particles, that leads to [oscillatory motions](#) of the medium.

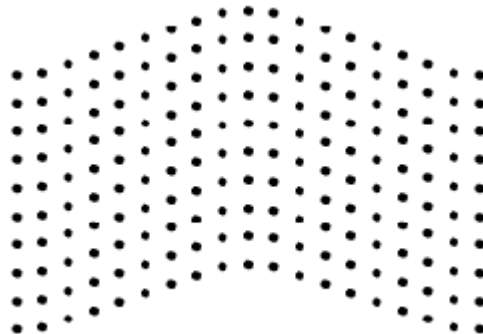
In solids, sound waves can propagate in four principle modes that are based on the way the particles oscillate. Sound can propagate as longitudinal waves, shear waves, surface waves, and in thin materials as plate waves. Longitudinal and shear waves are the two modes of propagation most widely used in ultrasonic testing. The particle movement responsible for the propagation of longitudinal and shear waves is illustrated below.



In [longitudinal waves](#), the oscillations occur in the longitudinal direction or the direction of wave propagation. Since compressional and dilational forces are active in these waves, they are also called pressure or compressional waves. They are also sometimes called density waves because their particle density fluctuates as they move. Compression waves can be generated in liquids, as well as solids because the energy travels through the atomic structure by a series of compression and expansion (rarefaction) movements



In the [transverse or shear wave](#), the particles oscillate at a right angle or transverse to the direction of propagation. Shear waves require an acoustically solid material for effective propagation and, therefore, are not effectively propagated in materials such as liquids or gasses. Shear waves are relatively weak when compared to longitudinal waves. In fact, shear waves are usually generated in materials using some of the energy from longitudinal waves.



## Modes of Sound Wave Propagation

In air, sound travels by compression and rarefaction of air molecules in the direction of travel. However, in solids, molecules can support vibrations in other directions, hence, a number of different types (modes) of sound waves are possible. As mentioned previously, longitudinal and transverse (shear) waves are most often used in ultrasonic inspection. However, at surfaces and interfaces, various types of elliptical or complex vibrations of the particles make other waves possible. Some of these wave modes such as Rayleigh and Lamb waves are also useful for ultrasonic inspection.

The table below summarizes many, but not all, of the wave modes possible in solids.

Wave Types in Solids	Particle Vibrations
Longitudinal	Parallel to wave direction
Transverse (Shear)	Perpendicular to wave direction
Surface - Rayleigh	Elliptical orbit - symmetrical mode
Plate Wave - Lamb	Component perpendicular to surface (extensional wave)
Plate Wave - Love	Parallel to plane layer, perpendicular to wave direction
Stoneley (Leaky Rayleigh Waves)	Wave guided along interface
Sezawa	Antisymmetric mode

Longitudinal and transverse waves were discussed on the previous page, so let's touch on surface and plate waves here.

Surface or Rayleigh waves travel the surface of a relative thick solid material penetrating to a depth of one wavelength. The particle movement has an elliptical orbit as shown in the image and animation below. Rayleigh waves are useful because they are very sensitive to surface defects and since they will follow the surface around, curves can also be used to inspect areas that other waves might have difficulty reaching.

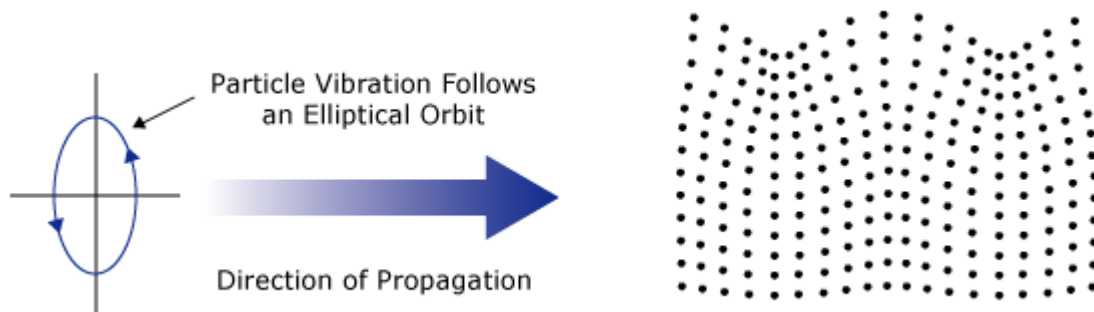
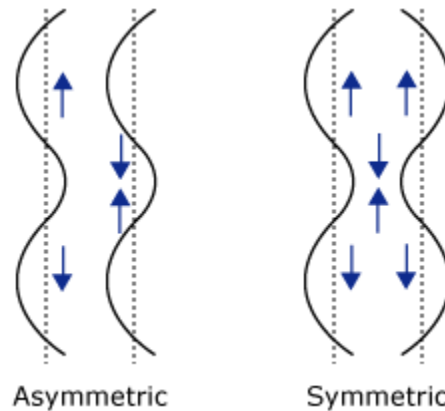


Plate waves can be propagated only in very thin metals. Lamb waves are the most commonly used plate waves in NDT. Lamb waves are a complex vibrational wave that travels through the entire thickness of a material. Propagation of Lamb waves depends on density, elastic, and material properties of a component, and they are influenced by a great deal by selected frequency and material thickness. With Lamb waves, a number of modes of particle vibration are possible, but the two most common are symmetrical and asymmetrical. The complex motion of the particles is similar to the elliptical orbits for surface waves.



## Wavelength and Defect Detection

In ultrasonic testing the inspector must make a decision about the frequency of the transducer that will be used. As we learned on the previous page, changing the frequency when the sound velocity is fixed will result in a change in the wavelength of the sound. The wavelength of the ultrasound used has significant affect on the probability of detecting a discontinuity. A rule of thumb in industrial inspections is that discontinuities that are larger than one-half the size of wavelength can be usually be detected.

Sensitivity and resolution are two terms that are often used in ultrasonic inspection to describe a technique's ability to locate flaws. Sensitivity is the ability to locate small discontinuities. Sensitivity generally increases with higher frequency (shorter wavelengths). Resolution is the ability of the system to locate discontinuities that are close together within the material or located near the part surface. Resolution also generally increases as the frequency increases.

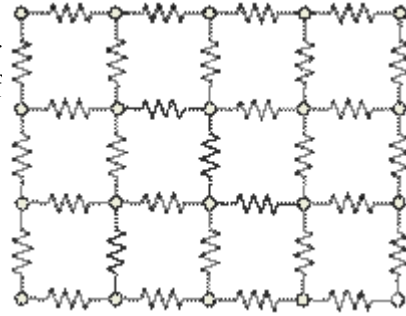
The wave frequency can also affect the capability of an inspection in adverse ways. Therefore, selecting the optimal inspection frequency often involves maintaining a balance between favorable and unfavorable results of the selection. Before selecting an inspection frequency, the grain structure, material thickness, size, type, and probable location of the discontinuity should be considered. As frequency increases, sound tends to scatter from large or coarse grain structure and from small imperfections within a material. Cast materials often have coarse grains and other sound scatters that require lower frequencies to be used for evaluations of these products. Wrought and forged products with directional and refined grain structure, can usually be inspected with higher frequency transducers.

Since more things in a material are likely to scatter a portion of the sound energy at higher frequencies, the penetrating power (or the maximum depth in a material that flaws can be located) is also reduced. Frequency also has an effect on the shape of the ultrasonic beam. Beam spread, or the divergence of the beam from the center axis of the transducer, and how it is affected by frequency will be discussed later.

It should be mentioned, so as not to be misleading, that a number of other variables will also affect the ability of ultrasound to locate defects. These include pulse length, type and voltage applied to the crystal, properties of the crystal, backing material, transducer diameter, and the receiver circuitry of the instrument. These are discussed in more detail in the material on signal-to-noise ratio.

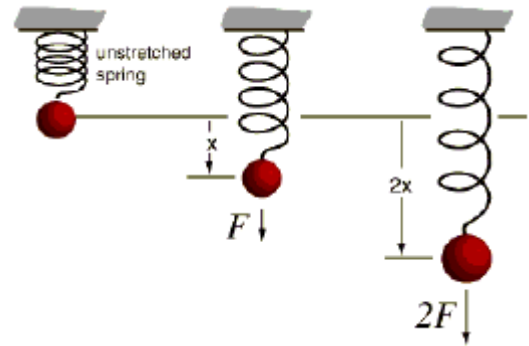
## Sound Propagation in Elastic Materials

In the previous pages, it was pointed out that sound waves propagate due to the vibrations or oscillatory motions of particles within a material. An ultrasonic wave may be visualized as an infinite number of oscillating masses or particles connected by means of elastic springs. Each individual particle is influenced by the motion of its nearest neighbor and both inertial and elastic restoring forces act upon each particle.



A mass on a spring has a single resonant frequency determined by its spring constant  $k$  and its mass  $m$ . The spring constant is the restoring force of a spring per unit of length. Within the elastic limit of any material, there is a linear relationship between the displacement of a particle and the force attempting to restore the particle to its equilibrium position. This linear dependency is described by **Hooke's Law**.

In terms of the spring model, Hooke's Law says that the restoring force due to a spring is proportional to the length that the spring is stretched, and acts in the opposite direction. Mathematically, Hooke's Law is written,  $F = -kx$ , where  $F$  is the force,  $k$  is the spring constant, and  $x$  is the amount of particle displacement. Hooke's law is represented graphically in the right. Please note that the spring is applying a force to the particle that is equal and opposite to the force pulling down on the particle.



## The Speed of Sound

Hooke's Law when used along with Newton's Second Law can explain a few things about the speed of sound. The speed of sound within a material is a function of the properties of the material and is independent of the amplitude of the sound wave. Newton's Second Law says that the force applied to a particle will be balanced by the particle's mass and the acceleration of the the particle. Mathematically, Newton's Second Law is written as  $F = ma$ . Hooke's Law then says that this force will be balanced by a force in the opposite direction that is dependent on the amount of displacement and the spring constant ( $F = -kx$ ). Therefore, since the applied force and the restoring force are equal,  $ma = -kx$  can be written. The negative sign indicates that the force is in the opposite direction.

Since the mass  $m$  and the spring constant  $k$  are constants for any given material, it can be seen that the acceleration  $a$  and the displacement  $x$ , are the only variables. It can also be seen that they are directly proportional. So if the displacement of the particle increases, so does its acceleration. It turns out that the time that it takes a particle to move and return to its equilibrium position is independent of the force applied. So, within a given material, sound always travels at the same speed no matter how much force is applied when other variables, such as temperature, are held constant.

### What properties of material affect its speed of sound?

Of course, sound does travel at different speeds in different materials. This is because the mass of the atomic particles and the spring constants are different for different materials. The mass of the particles is related to the density of the material, and the spring constant is related to the elastic constants of a material. The general relationship between the speed of sound in a solid and its density and elastic constants is given by the following equation:

$$V = \sqrt{\frac{C_{ij}}{\rho}}$$

Where  $V$  is the speed of sound,  $C$  is the elastic constant, and  $\rho$  is the material density. This equation may take a number of different forms depending on the type of wave (longitudinal or shear) and which of the elastic constants that are used. The typical elastic constants of a materials include:

- Young's Modulus,  $E$ : a proportionality constant between uniaxial stress and strain.
- Poisson's Ratio,  $\nu$ : the ratio of radial strain to axial strain
- Bulk modulus,  $K$ : a measure of the incompressibility of a body subjected to hydrostatic pressure.
- Shear Modulus,  $G$ : also called rigidity, a measure of substance's resistance to shear.
- Lamé's Constants,  $\lambda$  and  $\mu$ : material constants that are derived from Young's Modulus and Poisson's Ratio.

When calculating the velocity of a longitudinal wave, Young's Modulus and Poisson's Ratio are commonly used. When calculating the velocity of a shear wave, the shear modulus is used. It is often most convenient to make the calculations using Lamé's Constants, which are derived from Young's Modulus and Poisson's Ratio.

It must also be mentioned that the subscript  $ij$  attached to  $C$  in the above equation is used to indicate the directionality of the elastic constants with respect to the wave type and direction of wave travel. In isotropic materials, the elastic constants are the same for all directions within the material. However, most materials are anisotropic and the elastic constants differ with each direction. For example, in a piece of rolled aluminum plate, the grains are elongated in one direction and compressed in the others and the elastic constants for the longitudinal direction are different than those for the transverse or short transverse directions.

Examples of approximate compressional sound velocities in materials are:

- Aluminum - 0.632 cm/microsecond
- 1020 steel - 0.589 cm/microsecond
- Cast iron - 0.480 cm/microsecond.

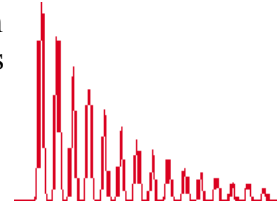
Examples of approximate shear sound velocities in materials are:

- Aluminum - 0.313 cm/microsecond
- 1020 steel - 0.324 cm/microsecond
- Cast iron - 0.240 cm/microsecond.

When comparing compressional and shear velocities it can be noted that shear velocity is approximately one half that of compressional. The sound velocities for a variety of materials can be found in the ultrasonic properties tables in the general resources section of this

## Attenuation of Sound Waves

When sound travels through a medium, its intensity diminishes with distance. In idealized materials, sound pressure (signal amplitude) is only reduced by the spreading of the wave. Natural materials, however, all produce an effect which further weakens the sound. This further weakening results from two basic causes, which are [scattering](#) and [absorption](#). The combined effect of scattering and absorption is called **attenuation**.



Attenuation of sound within a material itself is often not of intrinsic interest. However, natural properties and loading conditions can be related to attenuation. Attenuation often serves as a measurement tool that leads to the formation of theories to explain physical or chemical phenomenon, which decreases the ultrasonic intensity.

[Ultrasonic](#) attenuation is the decay rate of mechanical radiation at ultrasonic frequency as it propagates through material. A decaying [plane](#) wave is expressed as:

$$A = A_0 e^{-\alpha z}$$

In this expression  $A_0$  is the amplitude of the propagating wave at some location. The amplitude  $A$  is the reduced amplitude after the wave has traveled a distance  $Z$  from that initial location. The quantity  $\alpha$  is the attenuation coefficient of the wave traveling in the  $z$ -direction. The dimensions of  $\alpha$  are nepers/length, where a neper is a dimensionless quantity.  $e$  is Napier's constant which is equal to approximately 2.71828.

The units of the attenuation value in nepers/length can be converted to decibels/length by dividing by 0.1151. Decibels is a more common unit when relating the amplitudes of two signals.

Attenuation is generally proportional to the square of sound frequency. Quoted values of attenuation are often given for a single frequency, or an attenuation value averaged over many frequencies may be given. Also, the actual value of the attenuation coefficient for a given material is highly dependent on the way in which the material was manufactured. Thus, quoted values of attenuation only give a rough indication of the attenuation and should not be automatically trusted. Generally, a reliable value of attenuation can only be obtained by determining the attenuation experimentally for the particular material being used.

Attenuation can be determined by evaluating the multiple backwall reflections seen in a typical A-scan display like the one shown in the image above. The number of decibels between two adjacent signals is measured and this value is divided by the time interval between them. This calculation produces an attenuation coefficient in decibels per unit time  $U_t$ . This value can be converted to nepers/length by the following equation.

$$\alpha = \frac{0.1151}{v} U_t$$

Where  $v$  is the velocity of sound in meters per second and  $U_t$  is decibels per second.

## Acoustic Impedance

Sound travels through materials under the influence of sound pressure. Because molecules or atoms of a solid are bound elastically to one another, the excess pressure results in a wave propagating through the solid.

The **acoustic impedance (Z)** of a material is defined as the product of density (**p**) and acoustic velocity (**V**) of that material.

$$Z = pV$$

Acoustic impedance is important in

1. the determination of acoustic transmission and reflection at the boundary of two materials having different acoustic impedance
2. the design of ultrasonic transducers.
3. assessing absorption of sound in a medium.

The following figure will help you calculate the acoustic impedance for any material, so long as you know its density (p) and acoustic velocity (V). You may also compare two materials and "see" how they reflect and transmit sound energy. The red arrow represents energy of the reflected sound, while the blue arrow represents energy of the transmitted sound.

The reflected energy is the square of the difference divided by the sum of the acoustic impedances of the two materials.

$$R = \left( \frac{Z_2 - Z_1}{Z_2 + Z_1} \right)^2$$

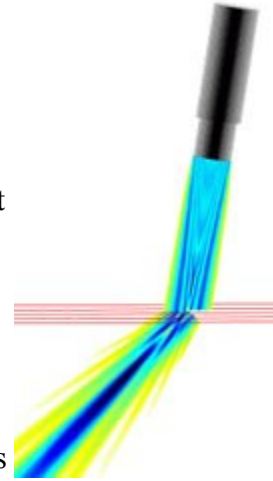
Note that Transmitted Sound Energy + Reflected Sound Energy = 1

## Reflection and Transmission Coefficients (Pressure)

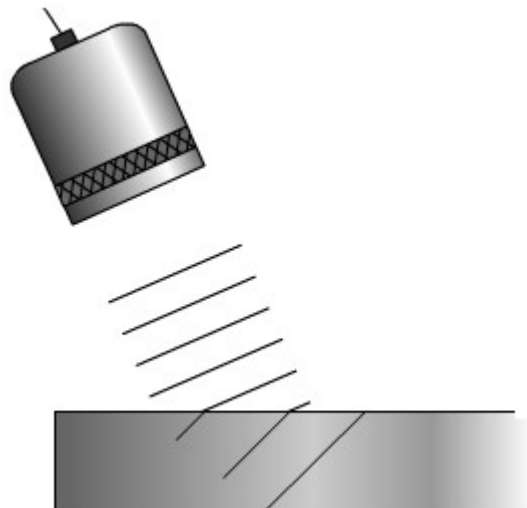
Ultrasonic waves are reflected at boundaries where there are differences in acoustic impedance, Z. This is commonly referred to as impedance mismatch. The fraction of the incident-wave intensity in reflected waves can be derived because particle velocity and local particle pressures are required to be continuous across the boundary between materials.

## Refraction and Snell's Law

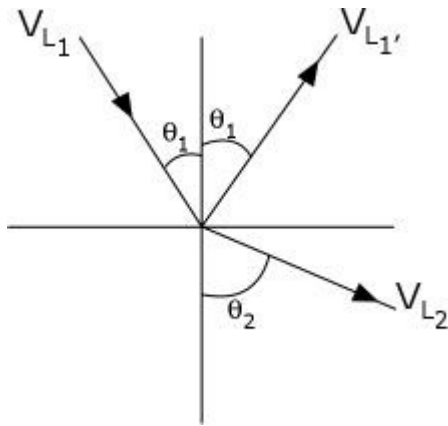
When an ultrasound wave passes through an interface between two materials at an oblique angle, and the materials have different indices of refraction, it produces both reflected and refracted waves. This also occurs with light and this makes objects you see across an interface appear to be shifted relative to where they really are. For example, if you look straight down at an object at the bottom of a glass of water, it looks closer than it really is. A good way to visualize how light and sound refract is to shine a flashlight into a bowl of slightly cloudy water noting the [refraction](#) angle with respect to the incidence angle.



Refraction takes place at an interface due to the different velocities of the acoustic waves within the two materials. The velocity of sound in each material is determined by the material properties (elastic modulus and density) for that material. In the animation below, a series of plane waves are shown traveling in one material and entering a second material that has a higher acoustic velocity. Therefore, when the wave encounters the interface between these two materials, the portion of the wave in the second material is moving faster than the portion of the wave in the first material. It can be seen that this causes the wave to bend.



Snell's Law describes the relationship between the angles and the velocities of the waves. Snell's law equates the ratio of material velocities  $v_1$  and  $v_2$  to the ratio of the **sine's** of incident ( $\theta_1$ ) and refraction ( $\theta_2$ ) angles, as shown in the following equation.



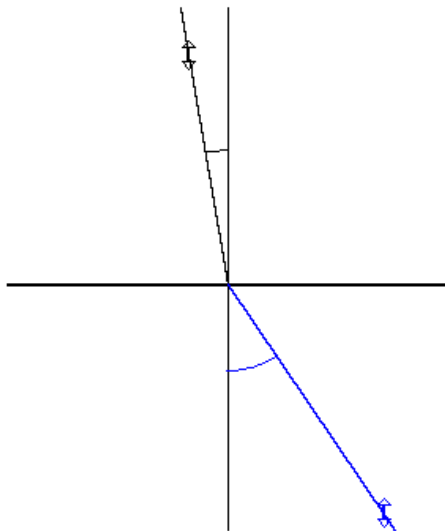
$$\frac{\sin\theta_1}{V_{L1}} = \frac{\sin\theta_2}{V_{L2}}$$

Where:

$V_{L1}$  is the longitudinal wave velocity in material 1.

$V_{L2}$  is the longitudinal wave velocity in material 2.

Water



\* Default units are cm/us, however, the user may assume other units.

Sin	<input type="text" value="10.000°"/>	v1	<input type="text" value="0.148"/>
=			
Sin	<input type="text" value="34.276°"/>	v2	<input type="text" value="0.48"/>

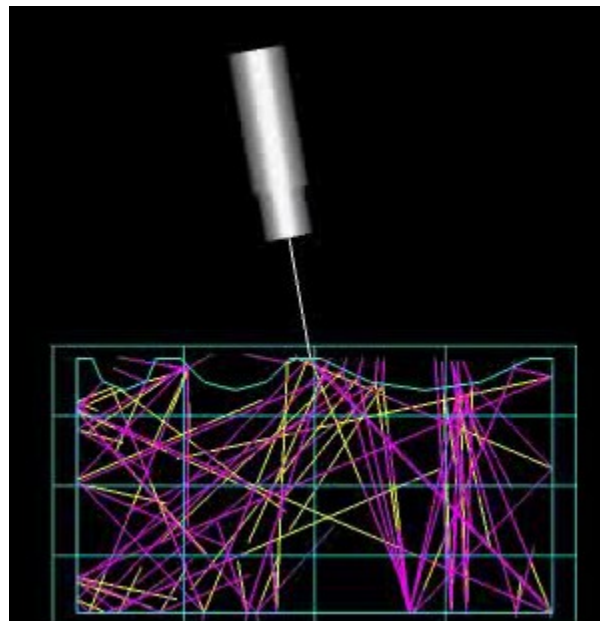
Material 2

Iron, Cast

When a longitudinal wave moves from a slower to a faster material, there is an incident angle that makes the angle of refraction for the wave  $90^\circ$ . This is known as the first critical angle. The first critical angle can be found from Snell's law by putting in an angle of  $90^\circ$  for the angle of the refracted ray. At the critical angle of incidence, much of the acoustic energy is in the form of an inhomogeneous compression wave, which travels along the interface and decays exponentially with depth from the interface. This wave is sometimes referred to as a "creep wave." Because of their inhomogeneous nature and the fact that they decay rapidly, creep waves are not used as extensively as Rayleigh surface waves in NDT. However, creep waves are sometimes useful because they suffer less from surface irregularities and coarse material microstructure, due to their longer wavelengths, than Rayleigh waves.

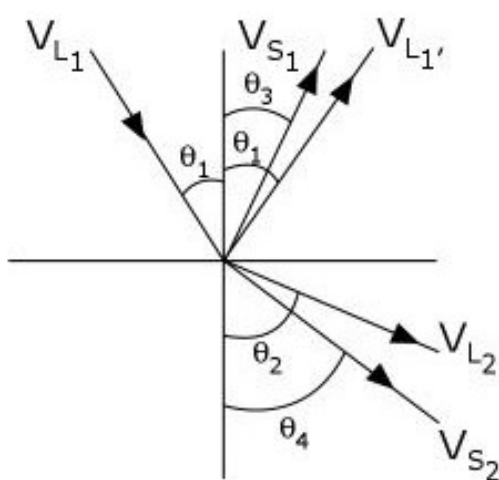
## Mode Conversion

When sound travels in a solid material, one form of wave energy can be transformed into another form. For example, when a longitudinal wave hits an interface at an angle, some of the energy can cause particle movement in the transverse direction to start a shear (transverse) wave. Mode conversion, occurs when a wave encounters an interface between materials of different acoustic impedance and the incident angle is not normal to the interface. From the ray tracing movie below it can be seen that since mode conversion occurs every time a wave encounters an interface at an angle, ultrasonic signals can become confusing at times.



In the previous section it was pointed out that when sound waves pass through an interface between materials having different acoustic velocities, refraction takes place at the interface. The larger the difference in acoustic velocities between the two materials, the more the sound is refracted. Notice that the shear wave is not refracted as much as the longitudinal wave. This occurs because shear waves travel slower than longitudinal waves. Therefore, the velocity difference between the incident longitudinal wave and the shear wave is not as great as it is between the incident and refracted longitudinal waves. Also note that when a longitudinal wave is reflected inside the material, the reflected shear wave is reflected at a smaller angle than the reflected longitudinal wave. This is also due to the fact that the shear velocity is less than the longitudinal velocity within a given material.

Snell's Law holds true for shear waves as well as longitudinal waves and can be written as follows.



$$\frac{\sin\theta_1}{V_{L1}} = \frac{\sin\theta_2}{V_{L2}} = \frac{\sin\theta_3}{V_{S1}} = \frac{\sin\theta_4}{V_{S2}}$$

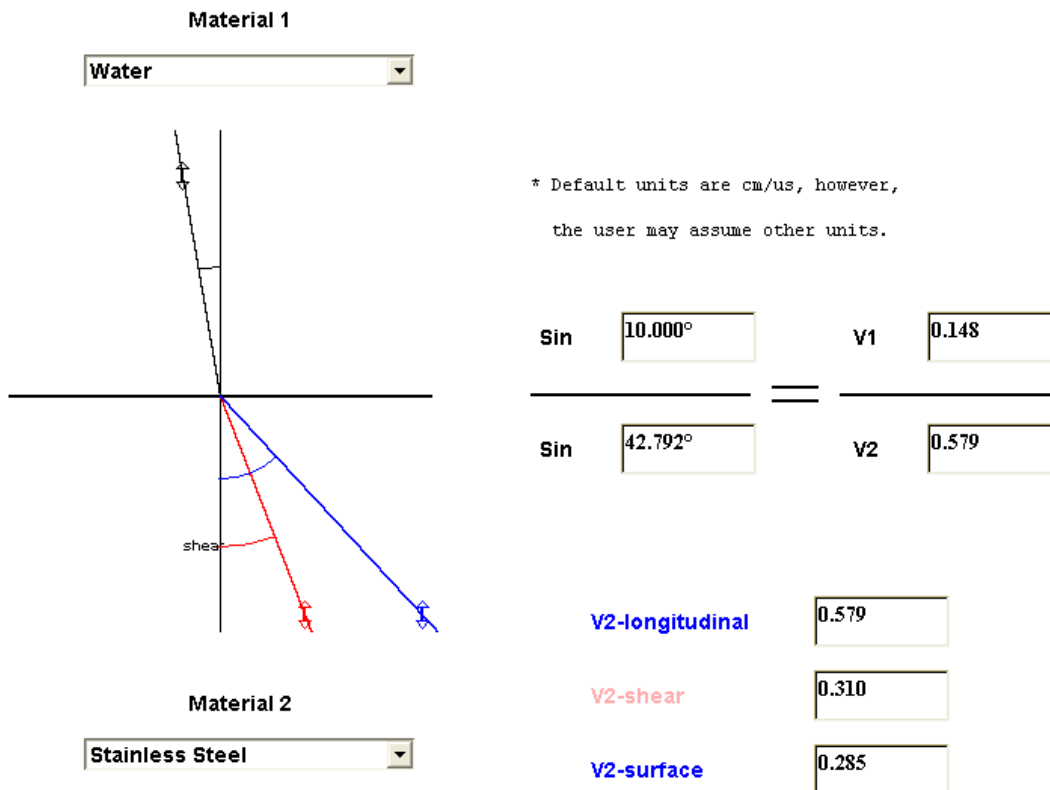
Where:

$V_{L1}$  is the longitudinal wave velocity in material 1.

$V_{L2}$  is the longitudinal wave velocity in material 2.

$V_{S1}$  is the shear wave velocity in material 1.

$V_{S2}$  is the shear wave velocity in material 2.



## Signal-to-Noise Ratio

In a previous page, the effect that frequency or wavelength has on flaw detectability was discussed. However, the detection of a defect involves many factors other than the relationship of wavelength and flaw size. For example, the amount of sound that reflects from a defect is also dependent acoustic impedance mismatch between the flaw and the surrounding material. A void is generally a better reflector than a metallic inclusion because the impedance mismatch is greater between air and metal than between metal and another metal. Often, the surrounding material has competing reflections. Microstructure grains in metals and the aggregate of concrete are a couple of examples. A good measure of detectability of a flaw is its signal-to-noise ratio (S/N). The signal-to-noise ratio is a measure of how the signal from the defect compares to other background reflections (categorized as "noise"). A signal to noise ratio of 3 to 1 is often required as a minimum. The absolute noise level and the absolute strength of an echo from a "small" defect depends on a number of factors:

- The probe size and focal properties.
- The probe frequency, bandwidth and efficiency.
- The inspection path and distance (water and/or solid).
- The interface (surface curvature and roughness).
- The flaw location with respect to the incident beam.
- The inherent noisiness of the metal microstructure.
- The inherent reflectivity of the flaw which is dependent on its acoustic impedance, size, shape, and orientation.
- Cracks and volumetric defects can reflect ultrasonic waves quite differently. Many cracks are "invisible" from one direction and strong reflectors from another.
- Multifaceted flaws will tend to scatter sound away from the transducer.

The following formula relates some of the variables affecting the signal-to-noise ratio (S/N) of a defect:

$$\frac{S}{N} = \sqrt{\frac{16}{\rho v_{metal} w_x w_y \Delta t}} \frac{A_{flaw}(f_0)}{FOM(f_0)}$$

The diagram shows the formula  $\frac{S}{N} = \sqrt{\frac{16}{\rho v_{metal} w_x w_y \Delta t}} \frac{A_{flaw}(f_0)}{FOM(f_0)}$  with the following labels:

- $\rho$ : sound speed in metal
- $v_{metal}$ : lateral beam widths at flaw depth
- $w_x$ : lateral beam widths at flaw depth
- $w_y$ : lateral beam widths at flaw depth
- $\Delta t$ : pulse duration
- $A_{flaw}(f_0)$ : Flaw scat. ampl. at center frequency
- $FOM(f_0)$ : Noise FOM at center frequency

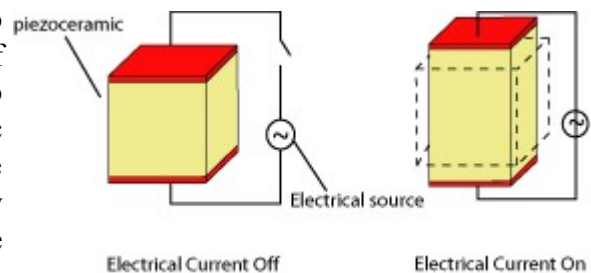
Rather than go into the details of this formulation, a few fundamental relationships can be pointed out. The signal-to-noise ratio (S/N), and therefore the detectability of a defect

- increases with increasing flaw size (scattering amplitude). The detectability of a defect is directly proportional to its size.
- increases with a more focused beam. In other words, flaw detectability is inversely proportional to the transducer beam width.
- increases with decreasing pulse width (delta-t). In other words, flaw detectability is inversely proportional to the duration of the pulse produced by an ultrasonic transducer. The shorter the pulse (often higher frequency), the better the detection of the defect. Shorter pulses correspond to broader bandwidth frequency response. See the figure below showing the waveform of a transducer and its corresponding frequency spectrum.

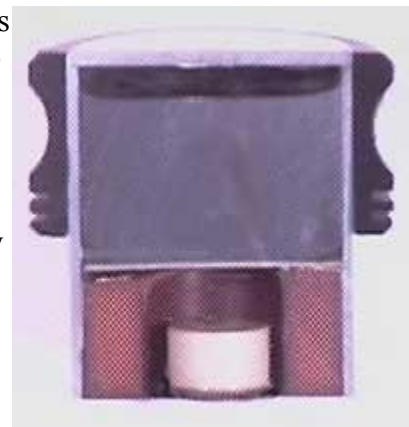
- decreases in materials with high density and/or a high ultrasonic velocity. The signal-to-noise ratio (S/N) is inversely proportional to material density and acoustic velocity.
- generally increases with frequency. However, in some materials, such as titanium alloys, both the " $A_{flaw}$ " and the "Figure of Merit (FOM)" terms in the equation change with about rate with changing frequency. So, in some cases, the signal-to-noise ratio (S/N) can be somewhat independent of frequency.

## Piezoelectric Transducers

The conversion of electrical pulses to mechanical vibrations and the conversion of returned mechanical vibrations back into electrical energy is the basis for ultrasonic testing. The active element is the heart of the transducer as it converts the electrical energy to acoustic energy, and vice versa. The active element is basically a piece polarized material (i.e. some parts of the molecule are positively charged, while other parts of the molecule are negatively charged) with electrodes attached to two of its opposite faces. When an electric field is applied across the material, the polarized molecules will align themselves with the electric field, resulting in induced dipoles within the molecular or crystal structure of the material. This alignment of molecules will cause the material to change dimensions. This phenomenon is known as electrostriction. In addition, a permanently-polarized material such as quartz ( $\text{SiO}_2$ ) or barium titanate ( $\text{BaTiO}_3$ ) will produce an electric field when the material changes dimensions as a result of an imposed mechanical force. This phenomenon is known as the piezoelectric effect. Additional information on why certain materials produce this effect can be found in the linked presentation material, which was produced by the Valpey Fisher Corporation.



The active element of most acoustic transducers used today is a [piezoelectric](#) ceramics, which can be cut in various ways to produce different wave modes. A large piezoelectric ceramic element can be seen in the image of a sectioned low frequency transducer. Preceding the advent of piezoelectric ceramic in the early 1950's, piezoelectric crystals made from quartz crystals and [magnetostrictive](#) materials were primarily used. The active element is still sometime referred to as the crystal by old timers in the NDT field.. When piezoelectric ceramics were introduced they soon became the dominant material for transducers due to their good piezoelectric properties and their ease of manufacture into a variety of

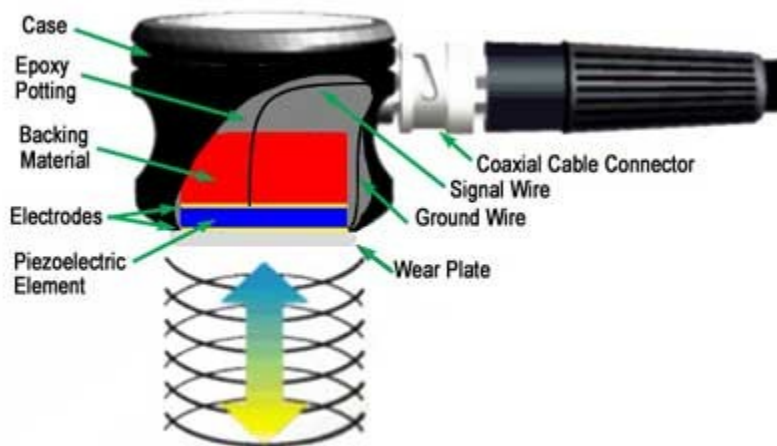


shapes and sizes. They also operate at low voltage and are usable up to about 300°C. The first piezoceramic in general use was barium titanate, and that was followed during the 1960's by lead zirconate titanate compositions, which are now the most commonly employed ceramic for making transducers. New materials such as piezo polymers and composites are also being used in some applications.

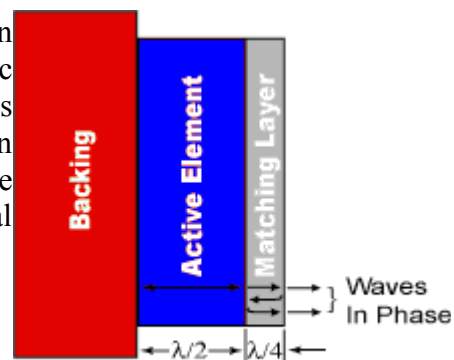
The thickness of the active element is determined by the desired frequency of the transducer. A thin wafer element vibrates with a wavelength that is twice its thickness. Therefore, piezoelectric crystals are cut to a thickness that is 1/2 the desired radiated wavelength. The higher the frequency of the transducer, the thinner the active element. The primary reason that high frequency contact transducers are not produced is because the element is very thin and too fragile.

## Characteristics of Piezoelectric Transducers

The transducer is an very important part of the ultrasonic instrumentation system. As discussed on the previous page, the transducer incorporates a piezoelectric element, which converts electrical signals into mechanical vibrations (transmit mode) and mechanical vibrations into electrical signals (receive mode). Many factors, including material, mechanical and electrical construction, and the external mechanical and electrical load conditions, influence the behavior a transducer. Mechanical construction includes parameters such as radiation surface area, mechanical damping, housing, connector type and other variables of physical construction. As of this writing, transducer manufactures are hard pressed when constructing two transducers that have identical performance characteristics.



A cut away of a typical contact transducer is shown above. It was previously learned that the piezoelectric element is cut to 1/2 the desired wavelength. To get as much energy out of the transducer as possible, an impedance matching is placed between the active element and the face of the transducer. Optimal



impedance matching is achieved by sizing the matching layer so that its thickness is  $1/4$  wavelength. This keeps waves that were reflected within the matching layer in phase when they exit the layer as illustrated in the image to the right. For contact transducers, the matching layer is made from a material that has an acoustical impedance between the active element and steel. Immersion transducers have a matching layer with an acoustical impedance between the active element and water. Contact transducers also often incorporate a wear plate to protect the matching layer and active element from scratch.

The backing material supporting the crystal has a great influence on damping characteristics of a transducer. Using a backing material with an impedance similar to that of the active element will produce the most effective damping. Such a transducer will have a narrow bandwidth resulting in higher sensitivity. As the mismatch in impedance between the active element and the backing material increases, material penetration increased but transducer sensitivity is reduced.

### **Transducer Efficiency, Bandwidth and Frequency**

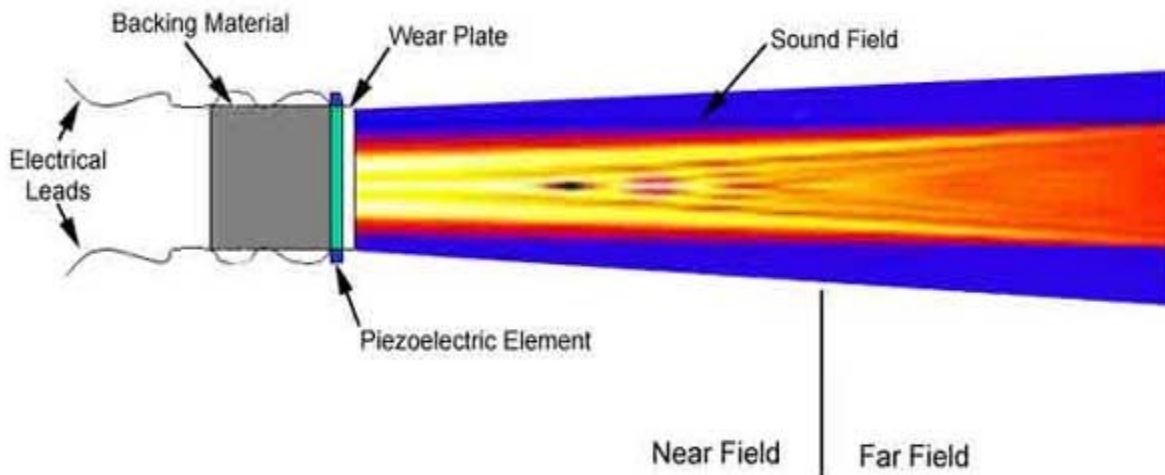
Some transducers are specially fabricated to be more efficient transmitters and others to be more efficient receivers. A transducer that performs well in one application will not always produce the desired results in a different application. For example, sensitivity to small defects is proportional to the product of the efficiency of the transducer as a transmitter and a receiver. Resolution, the ability to locate defects near surface or in close proximity in the material, requires a highly damped transducer.

It is also important to understand the concept of bandwidth, or range of frequencies, associated with a transducer. The frequency noted on a transducer is the central or center frequency and depends primarily on the backing material. Highly damped transducers will respond to frequencies above and below the central frequency. The broad frequency range provides a transducer with high resolving power. Less damped transducers will exhibit a narrower frequency range, poorer resolving power, but greater penetration. The central frequency will also define capabilities of a transducers. Lower frequencies (0.5Mhz-2.25Mhz) provide greater energy and penetration in a material, while high frequency crystals (15.0Mhz-25.0Mhz) provide reduced penetration but greater sensitivity to small discontinuities. High Frequency Transducers, when used with the proper instrumentation, can improve flaw resolution and thickness measurement capabilities dramatically. Broadband transducers with frequencies up to 150 MHz are commercially available.

Transducers are constructed to withstand some abuse, but they should be handled carefully. Misuse such as dropping can cause cracking of the wear plate, element, or the backing material. Damage to a transducer is often noted on the a-scan presentation as an enlargement of the initial pulse.

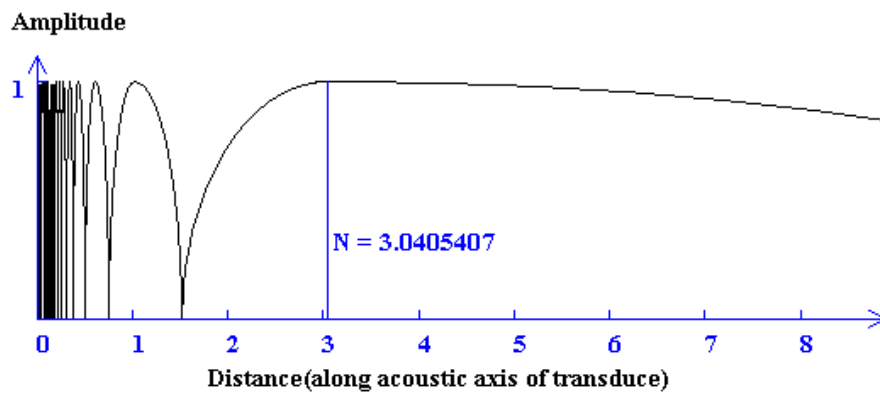
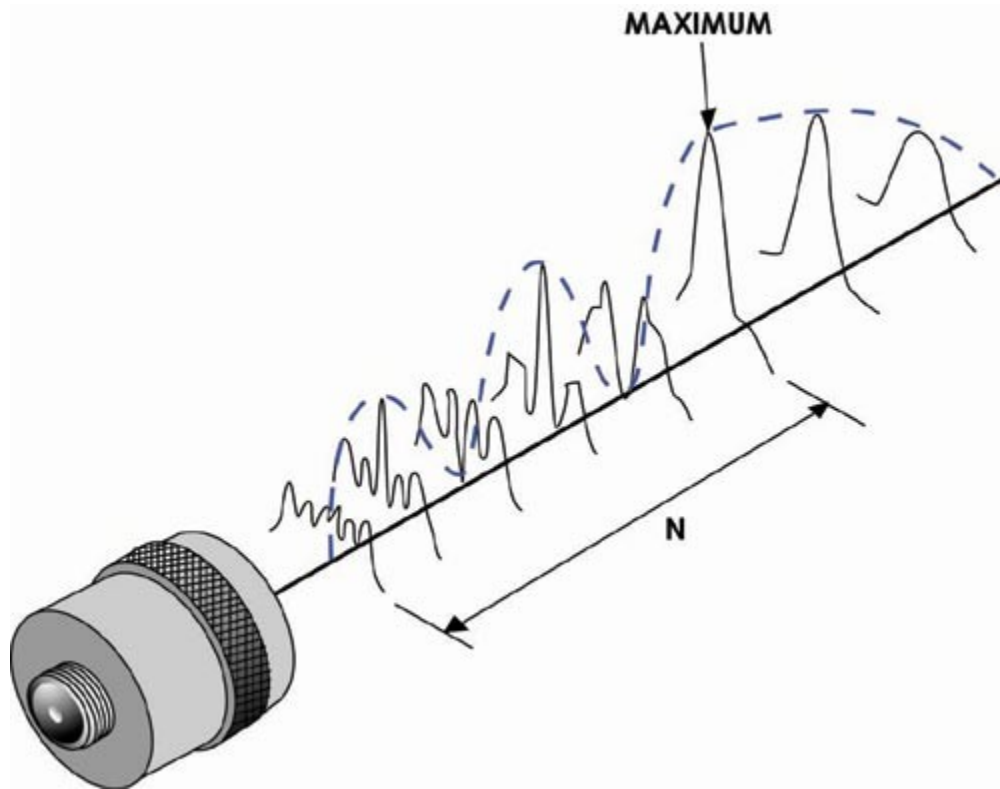
## Radiated Fields of Ultrasonic Transducers

The sound that emanates from a piezoelectric transducer does not originate from a point, but instead originates from most of the surface of the piezoelectric element. Round transducers are often referred to as piston source transducers because the sound field resembles a cylindrical mass in front of the transducer. The sound field from a typical piezoelectric transducer is shown below. The intensity of the sound is indicated by color, with lighter colors indicating higher intensity.



Since the ultrasound originates from a number of points along the transducer face, the ultrasound intensity along the beam is affected by constructive and destructive wave interference as discussed in a previous page on [wave interference](#). These are sometimes also referred to as [diffraction](#) effects in the NDT world. There are extensive fluctuations near the source, known as the near field. These high and low pressure areas are generated because the crystal is not a point source of sound pressure, but rather a series of high and low pressure waves which are joined into a uniform front at the end of the near zone. Because of acoustic variations within a near field, it can be extremely difficult to accurately evaluate flaws in materials when they are positioned within this area..

The ultrasonic beam is more uniform in the far field, where the beam spreads out in a pattern originating from the center of the transducer. The transition between these zones occurs at a distance,  $N$ , and is sometimes referred to as the "natural focus" of a flat ( or unfocused ) transducer. The near/far distance,  $N$ , is significant because amplitude variations that characterize the near field change to a smoothly declining amplitude at this point. This area just beyond the near field is where the sound wave is well behaved and at its maximum strength. Therefore, optimal detection results will be obtained when flaws occur in this area.



$$N \text{ } \boxed{3.040} = \frac{a \text{ } \boxed{0.300}^2 * \text{freq } \boxed{5.000}}{v \text{ } \boxed{0.148}}$$

## Transducer Beam Spread

As discussed on the previous page, round transducers are often referred to as piston source transducers because the sound field resembles a cylindrical mass in front of the transducer. However, the energy in the beam does not remain in a cylinder, but instead spread out as it propagates through the material. The phenomenon is usually referred to as beam spread but is sometimes also called beam divergence or ultrasonic diffraction. Although beam spread must be considered when performing an ultrasonic inspection, it is important to note that in the far field, or [Fraunhofer](#) zone, the maximum sound pressure is always found along the acoustic axis (centerline) of the transducer. Therefore, the strongest reflection are likely to come from the area directly in front of the transducer.

Beam spread occurs because the vibrating particle of the material (through which the wave is traveling) do not always transfer all of their energy in the direction of wave propagation. Recall that waves propagate through that transfer of energy from one particle to another in the medium. If the particles are not directly aligned in the direction of wave propagation, some of the energy will get transferred off at an angle. (Picture what happens when one ball hits another second ball slightly off center). In the near field constructive and destructive wave interference fill the sound field with fluctuation. At the start of the far field, however, the beam strength is always greatest at the center of the beam and diminishes as it spreads outward.

As shown in the applet below, beam spread is largely determined by the frequency and diameter of the transducer. Beam spread is greater when using a low frequency transducer than when using a high frequency transducer. As the diameter of the transducer increases the beam spread will be reduced.

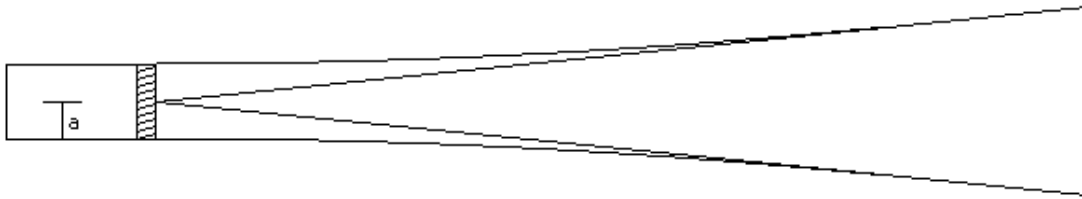
Beam angle is an important consideration in transducer selection for a couple of reasons. First, beam spread lowers the amplitude of reflections since sound fields are less concentrated and, therefore, weaker. Second, beam spread may result in more difficult to interpret signals due to reflections from the lateral sides of the test object or other features outside of the inspection area. Characterization of the sound field generated by a transducer is a prerequisite to understanding observed signals.

Numerous codes exist that can be used to standardize the method used for the characterization of beam spread. American Society for Testing and Materials method number ASTM E-1065, addresses methods for ascertaining beam shapes in Section A6, Measurement of Sound Field Parameters. However, these measurements are limited to immersion probes. In fact, the methods described in E-1065 are primarily concerned with the measurement of beam characteristics in water, and as such are limited to measurements of the compression mode only. Techniques described in E-1065 include pulse-echo using a ball target and hydrophone receivers, which allows the sound field of the probe to be assessed for the entire volume in front of the probe.

For a flat piston source transducer, an approximation of the beam shape may be calculated as a function of radius (**a**), frequency (**f**), and velocity (**V**) of a liquid or solid medium. The applet below allows the user to calculate the beam spread angle which

represents a falling of of sound pressure (intensity) to the side of the acoustic axis of one half (-6 dB) as a function of transducer parameters radius and frequency and as a function of acoustic velocity in a medium.

**Beam Spread (-6dB)**

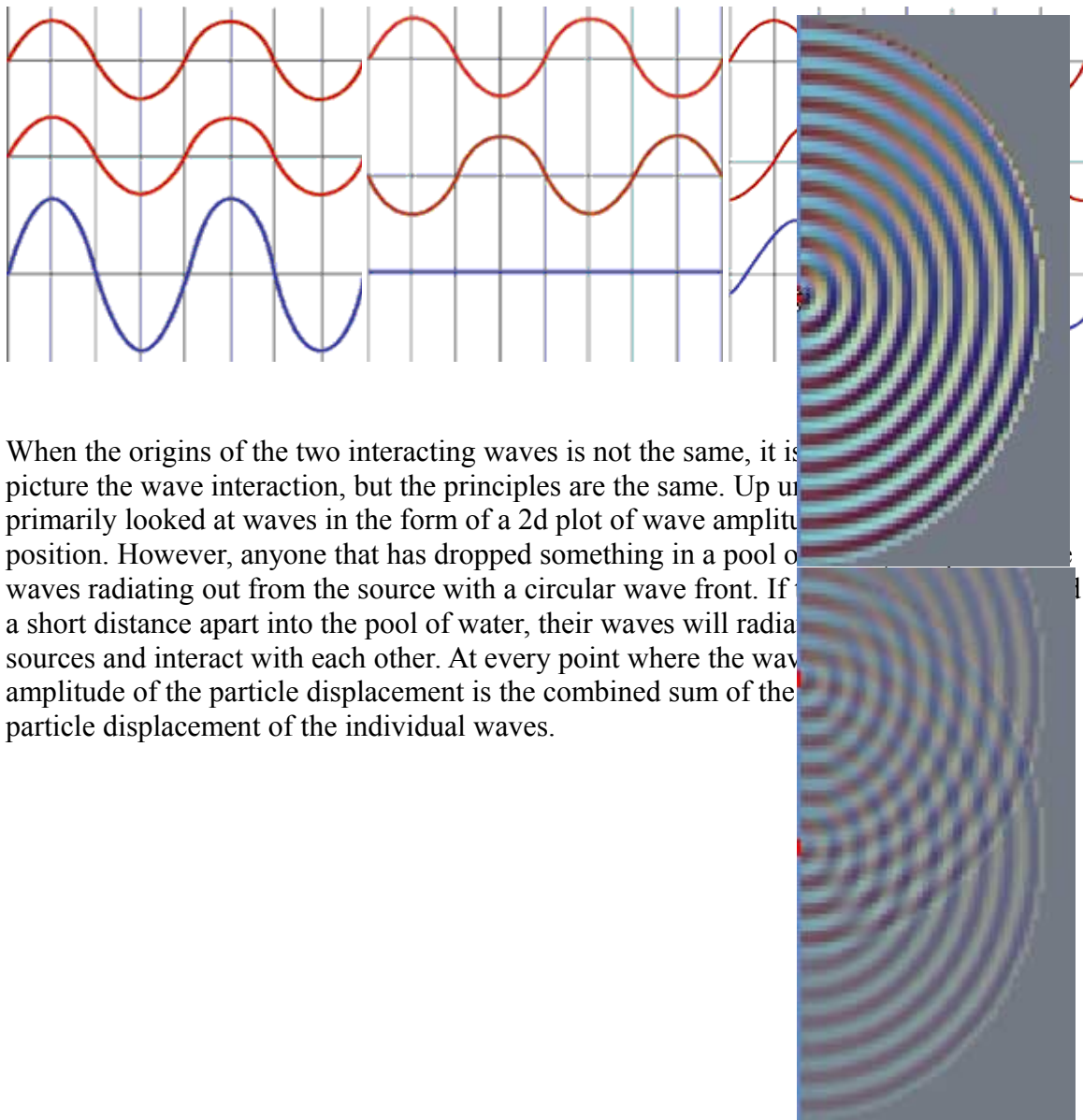


$$\sin \frac{2.906}{2} = \frac{0.514 * v \ 0.148}{2 * a \ 0.300 \ *freq \ 5.000}$$

## Wave Interaction or Interference

Before we move into the next section, the subject of wave interaction must be covered since it is important when trying to understand the performance of an ultrasonic transducer. On the previous pages, wave propagation was discussed as if a single sinusoidal wave was propagating through the material. However, the sound that emanates from an ultrasonic transducer does not originate from a single point, but instead originates from many points along the surface of the piezoelectric element. This results in a sound field with many waves interacting or interfering with each other.

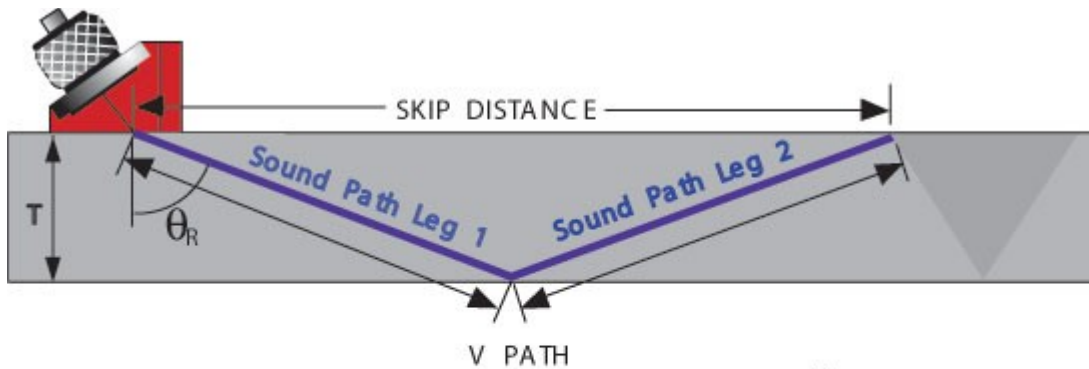
When waves interact, they superimpose on each other, and the amplitude of the sound pressure or particle displacement at any point of interaction is the sum of the amplitudes of the two individual waves. First, let's consider two identical waves that originate from the same point. When they are *in phase* (so that the peaks and valleys of one are exactly aligned with those of the other), they combine to double the displacement of either wave acting alone. When they are completely *out of phase* (so that the peaks of one wave are exactly aligned with the valleys of the other wave), they combine to cancel each other out. When the two waves are not completely *in phase* or *out of phase*, the resulting wave is the sum of the wave amplitudes for all points along the wave.



When the origins of the two interacting waves is not the same, it is picture the wave interaction, but the principles are the same. Up until now we have primarily looked at waves in the form of a 2d plot of wave amplitude versus position. However, anyone that has dropped something in a pool of water has seen waves radiating out from the source with a circular wave front. If you drop two stones a short distance apart into the pool of water, their waves will radiate from two sources and interact with each other. At every point where the waves meet, the amplitude of the particle displacement is the combined sum of the amplitudes of the individual waves.

## Angle Beams II

Angle Beam Transducers and wedges are typically used to introduce a refracted shear wave into the test material. The geometry of the sample below allows the sound beam to be reflected from the back wall to improve detectability of flaws in and around welded areas.



$\theta_R$  = Refracted Angle

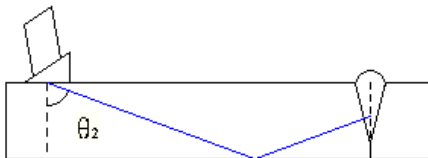
T = Material Thickness

Skip Distance =  $2T \times \tan\theta_R$

$$\text{Leg} = \frac{T}{\cos\theta_R}$$

$$\text{V-Path} = \frac{2T}{\cos\theta_R}$$

Move Transducer With Mouse



Refracted Angle

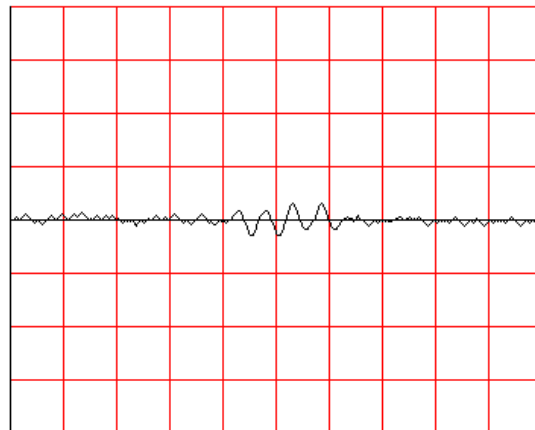
70.0°

Thickness = 1.000

Surface Distance = 4.263

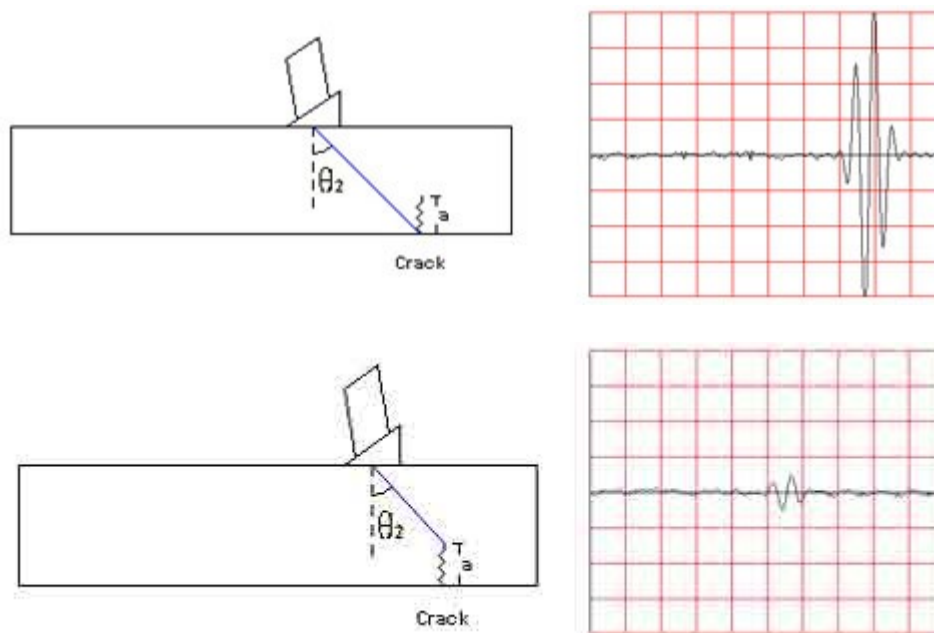
V-Path = 4.537

Dept (2nd Leg) = 0.446

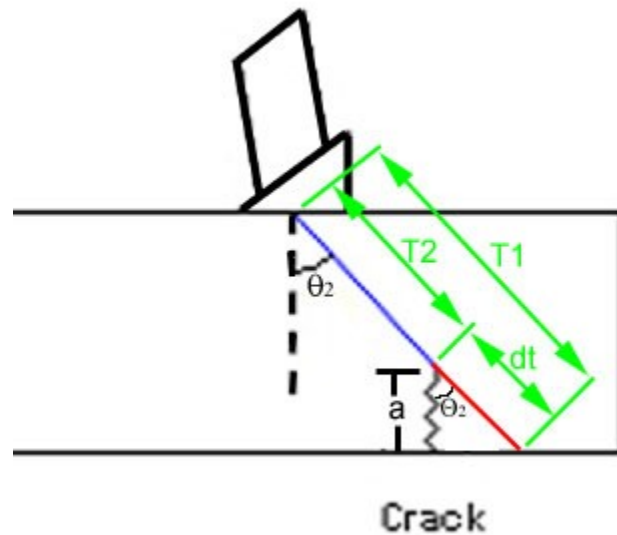


## Crack Tip Diffraction

When the geometry of the part is relatively uncomplicated and the orientation of a flaw is well known, the length ( $a$ ) of a crack can be determined by a technique known as [tip diffraction](#). One common application of the tip diffraction technique is to determine the length of a crack originating from on the backside of a flat plate as shown below. In this case, when an angle beam transducer is scanned over the area of the flaw, the principle echo comes from the base of the crack to locate the position of the flaw (Image 1). A second, much weaker echo comes from the tip of the crack and since the distance traveled by the ultrasound is less, the second signal appears earlier in time on the scope (Image 2).



Crack height ( $a$ ) is a function of the ultrasound velocity ( $v$ ) in the material, the incident angle ( $\Theta_2$ ), and the difference in arrival times between the two signals ( $dt$ ). Since the incident angle and the thickness of the material is the same in both measurements, two similar right triangles are formed such that one can be overlaid on the other. A third similar right triangle is made, which is comprised on the crack, the length  $dt$  and the angle  $\Theta_2$ . The variable  $dt$  is really the difference in time but can easily be converted to a distance by dividing the time in half (to get the one-way travel time) and multiplying this value by the velocity of the sound in the material. Using trigonometry an equation for estimating crack height from these variables can be derived as shown below.



$$\text{Cos } \theta = \frac{\text{Distance } a}{\text{Distance } dt}$$

Solving for "a" the equation becomes

$$a = \text{Cos } \theta \times (\text{Distance } dt)$$

The equation is complete once distance dt is calculated by dividing the difference in time between the two signals (dt) by two and multiplying this value by the sound velocity.

$$a = \text{Cos } \theta \times \frac{(dt \times v)}{2}$$

## Automated Scanning

Ultrasonic scanning systems are used for automated data acquisition and imaging. They typically integrate an ultrasonic instrumentation, a scanning bridge, and computer controls. The signal strength and/or the time-of-flight of the signal is measured for every point in the scan plan. The value of the data is plotted using colors or shades of gray to produce detailed images of the surface or internal features of a component. Systems are usually capable of displaying the data in A-, B- and C-scan modes simultaneously. With any ultrasonic scanning system there are two factors to consider:

1. how to generate and receive the ultrasound.
2. how to scan the transducer(s) with respect to the part being inspected.

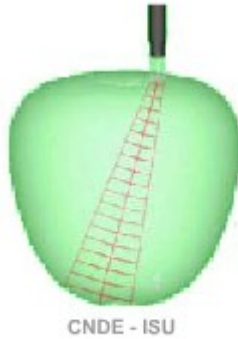


The most common ultrasonic scanning systems involve the use of an immersion tank as shown in the image above. The ultrasonic transducer and the part are placed under water so that consistent coupling is maintained by the water path as the transducer or part is moved within the tank. However, scanning systems come in a large variety of configurations to meet specific inspection needs. In the image to the right, an engineer aligns the heads of a squirter system that uses a through-transmission technique to inspect aircraft composite structures. In this system, the ultrasound travels through columns of forced water which are scanned about the part with a robotic system. A variation of the squirter system is the "Dripless Bubbler" scanning system, which is discussed below.



It is often desirable to eliminate the need for the water coupling and a number of state-of-the-art UT scanning systems have done this. Laser ultrasonic systems use laser beams to generate the ultrasound and collect the resulting signals in a noncontact mode. Advances in transducer technology has led to the development of an inspection technique known as air-coupled ultrasonic inspection. These systems are capable of sending ultrasonic energy through air and getting enough energy into the part to have a useable signal. These system typically use a through-transmission technique since reflected energy from discontinuities are too weak to detect.

The second major consideration is how to scan the transducer(s) with respect to the part being inspected. When the sample being inspected has a flat surface, a simple raster-scan can be performed. If the sample is cylindrical, a turntable can be used to turn the sample while the transducer is held stationary or scanned in the axial direction of the cylinder. When the sample is irregular shaped, scanning becomes more difficult. As illustrated in the beam modeling animation, curved surface can steer, focus and defocus the ultrasonic beam. For inspection applications involving parts having complex curvatures, scanning systems capable of performing contour following are usually necessary.



## Precision Velocity Measurements

Changes in ultrasonic wave propagation speed, along with energy losses, from interactions with a material's microstructures are often used to nondestructively gain information about a material's properties. Measurements of sound velocity and ultrasonic wave attenuation can be related to the elastic properties that can be used to characterize the texture of polycrystalline metals. These measurements enable industry to replace destructive microscopic inspections with nondestructive methods.

Of interest in velocity measurements are [longitudinal wave](#), which propagate in gases, liquids, and solids. In solids, also of interest are [transverse \(shear\) waves](#). The longitudinal velocity is independent of sample geometry when the dimensions at right angles to the beam are large compared to the beam area and wavelength. The transverse velocity is affected little by the physical dimensions of the sample.

### Pulse-Echo and Pulse-Echo-Overlap Methods

Rough ultrasonic velocity measurements are as simple as measuring the time it takes for a pulse of ultrasound to travel from one transducer to another (pitch-catch) or return to the same transducer (pulse-echo). Another method is to compare the phase of the detected sound wave with a reference signal: slight changes in the transducer separation are seen as slight phase changes, from which the sound velocity can be calculated. These methods are suitable for estimating acoustic velocity to about 1 part in 100. Standard practice for measuring velocity in materials is detailed in ASTM E494.

### Precision Velocity Measurements (using EMATs)

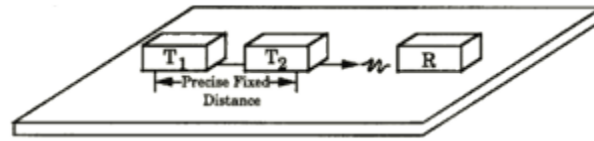
Electromagnetic-acoustic transducers (EMAT) generate ultrasound in the material being investigated. When a wire or coil is placed near to the surface of an electrically conducting object and is driven by a current at the desired ultrasonic frequency, eddy currents will be induced in a near surface region. If a static magnetic field is also present, these currents will experience Lorentz forces of the form

$$\mathbf{F} = \mathbf{J} \times \mathbf{B}$$

where  $\mathbf{F}$  is a body force per unit volume,  $\mathbf{J}$  is the induced dynamic current density, and  $\mathbf{B}$  is the static magnetic induction.

The most important application of EMATs has been in nondestructive evaluation (NDE) applications such as flaw detection or material property characterization. Couplant free transduction allows operation without contact at elevated temperatures and in remote locations. The coil and magnet structure can also be designed to excite complex wave patterns and polarizations that would be difficult to realize with fluid coupled piezoelectric probes. In the inference of material properties from precise velocity or attenuation measurements, use of EMATs can eliminate errors associated with couplant variation, particularly in contact measurements.

Differential velocity is measured using a T<sub>1</sub>-T<sub>2</sub>---R fixed array of EMAT [transducers](#) at 0, 45°, 90° or 0°, 90° relative rotational directions depending on device configuration:



	Texture	Stress	
Ferrous	0, 45, 90	0, 90	Pulsed Magnets
Non-Ferrous	0, 45, 90	0, 90	Permanent Magnets
	$S_0$	$SH_0$	

**EMAT Driver Frequency: 450-600 KHz (nominal)**

**Sampling Period: 100 ns**

**Time Measurement Accuracy:**

Resolution 0.1 ns

Accuracy required for less than 2 KSI Stress Measurements: Variance 2.47 ns

Accuracy required for texture: Variance 10.0 ns

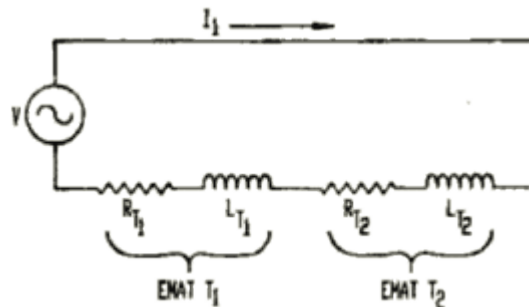
W440 < 3.72E-5

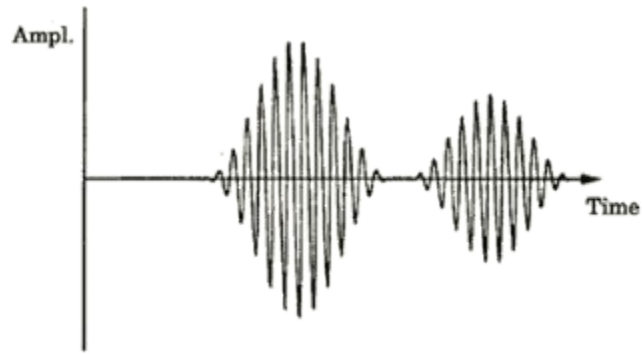
W420 < 1.47E-4

W400 < 2.38E-4

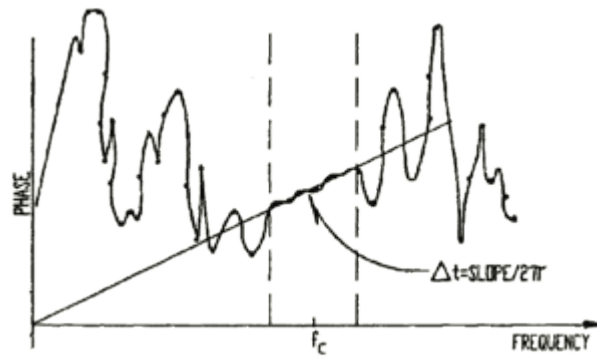
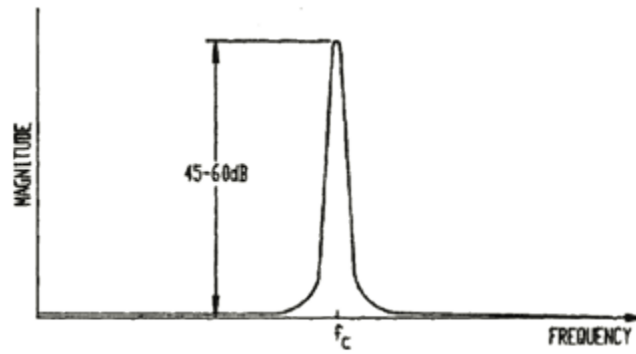
### Time Measurement Technique

Fourier Transform-Phase-Slope determination of delta time between received RF bursts (T<sub>2</sub>-R) - (T<sub>1</sub>-R), where T<sub>2</sub> and T<sub>1</sub> EMATs are driven in series to eliminate differential phase shift due to probe liftoff.





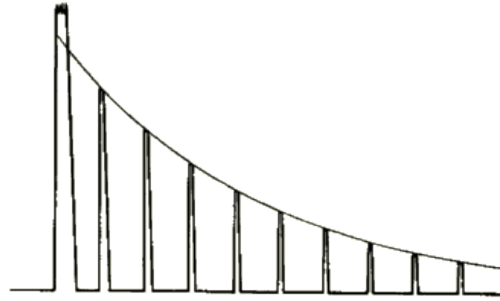
Received Waveforms from  $T_1$  and  $T_2$



Slope of the phase is determined by linear regression of weighted data points within the signal bandwidth and a weighted y-intercept. The accuracy obtained with this method can exceed one part in one hundred thousand (1:100,000).

## Attenuation Measurements

Ultrasonic wave propagation is influenced by the microstructure of the material through which it propagates. The velocity of the ultrasonic waves is influenced by the elastic moduli and the density of the material, which in turn are mainly governed by the amount of various phases present and the damage in the material. Ultrasonic attenuation, which is the sum of the absorption and the scattering, is mainly dependent upon the damping capacity and scattering from the grain boundary in the material. However, to fully characterize the attenuation required knowledge of a large number of thermo-physical parameters that in practice are hard to quantify.



Relative measurements such as the change of attenuation and simple qualitative tests are easier to make than absolute measure. Relative attenuation measurements can be made by examining the exponential decay of multiple back surface reflections. However, significant variations in microstructural characteristics and mechanical properties often produce only a relatively small change in wave velocity and attenuation.

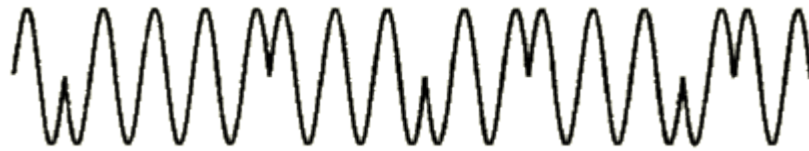
Absolute measurements of attenuation are very difficult to obtain because the echo amplitude depends on factors in addition to amplitude. The most common method used to get quantitative results is to use an ultrasonic source and detector transducer separated by a known distance. By varying the separation distance, the attenuation can be measured from the changes in the amplitude. To get accurate results, the influence of coupling conditions must be carefully addressed. To overcome the problems related to conventional ultrasonic attenuation measurements, ultrasonic spectral parameters for frequency-dependent attenuation measurements, which are independent from coupling conditions are also used. For example, the ratio of the amplitudes of higher frequency peak to the lower frequency peak, has been used for microstructural characterization of some materials.

## Spread Spectrum Ultrasonics

Spread [spectrum](#) ultrasonics makes use of the correlation of continuous signals rather than pulse-echo or pitch-catch techniques.

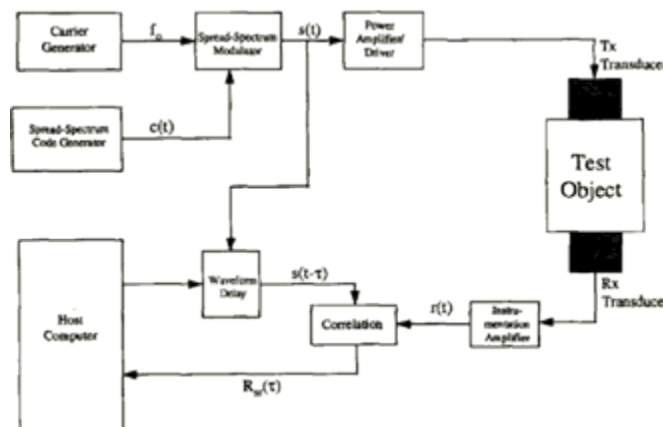
Spread spectrum ultrasonics is a patented new broad band spread-spectrum ultrasonic nondestructive evaluation method. In conventional ultrasonics, a pulse or tone burst is transmitted, then received echoes or through-transmission signals are received and analyzed.

In spread spectrum ultrasonics, encoded sound is continuously transmitted into the part or structure being tested. Instead of receiving echoes, spread spectrum ultrasonics generates an acoustic correlation signature having a one-to-one correspondence with the acoustic state of the part or structure (in its environment) at the instant of the measurement. In its simplest embodiment, the acoustic correlation signature is generated by cross correlating an encoding sequence, with suitable cross and auto correlation properties, transmitted into a part (structure) with received signals returning from the part (structure).



Section of biphasemodulated spread spectrum ultrasonic waveform

Multiple probes may be used to ensure that acoustic energy is propagated through all critical volumes of the structure. Triangulation may be incorporated with multiple probes to locate regions of detected distress. Spread spectrum ultrasonics can achieve very high sensitivity to acoustic propagation changes with a low level of energy.

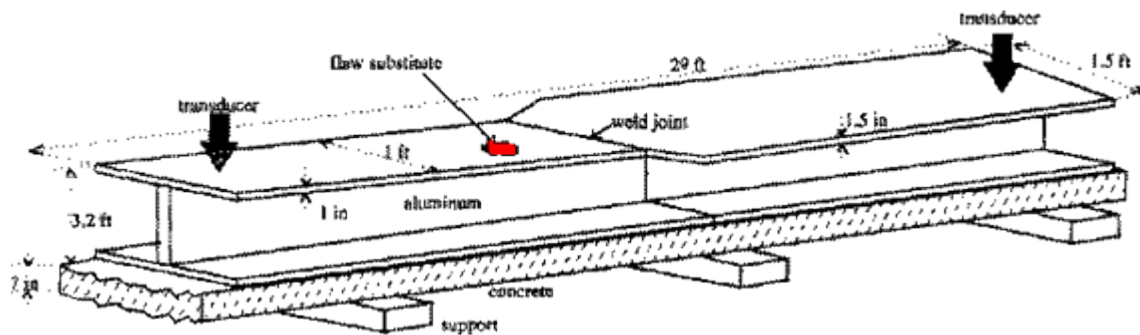


**Two significant applications of Spread Spectrum Ultrasonics are:**

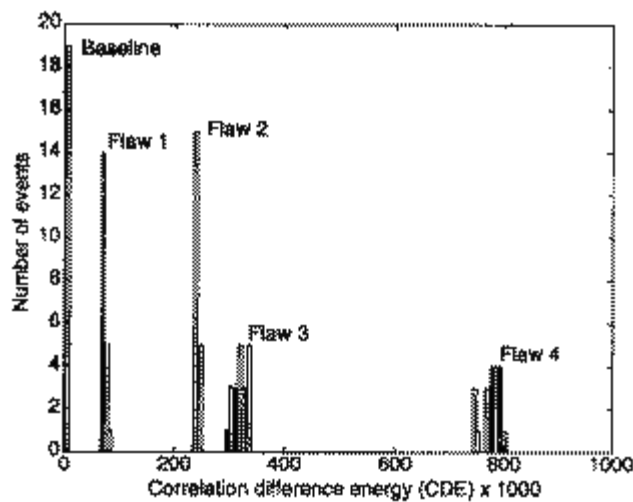
1. Large Structures that allow ultrasonic transducers to be "permanently" affixed to the structures, eliminating variations in transducer registration and couplant. Comparisons with subsequent acoustic correlation signatures can be used to monitor critical structures such as fracture critical bridge girders. In environments where structures experience a great many variables such as temperature, load, vibration, or environmental coupling, it is necessary to filter out these effects to obtain the correct measurements of defects.

In the example below, simulated defects were created by setting a couple of steel blocks on the top of the bridge girder.

Trial	Setup	Contact Area
Baseline	No Flaw	--
Flaw 1	One block laying flat on girder	12.5 sq in
Flaw 2	One block standing on its long side	1.25 sq in
Flaw 3	Both blocks standing on their long sides	2.50 sq in
Flaw 4	Both blocks laying flat on girder	25.0 sq in



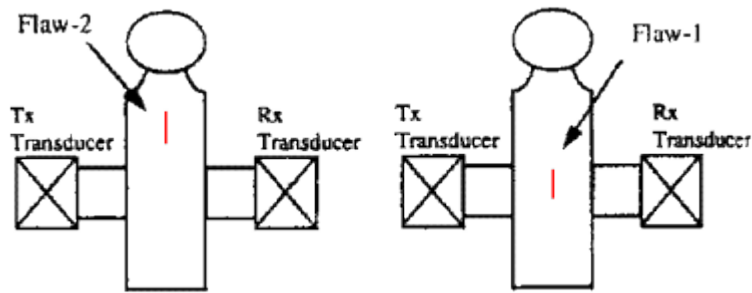
2. Piece-part environments transducers and be precisely eliminating variations in registration and Acoustic signatures may be compared to an known "good" or



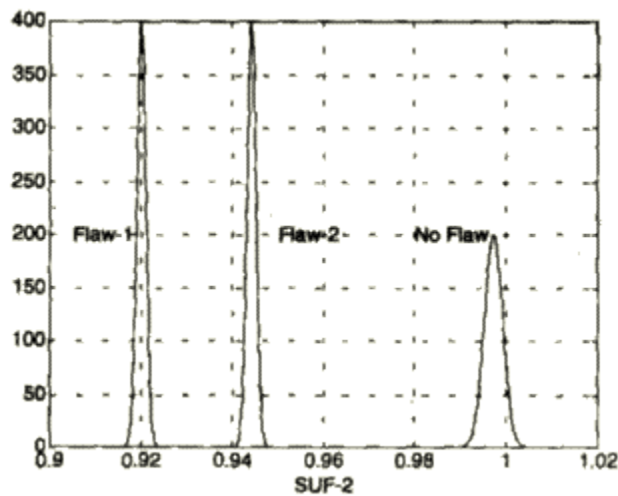
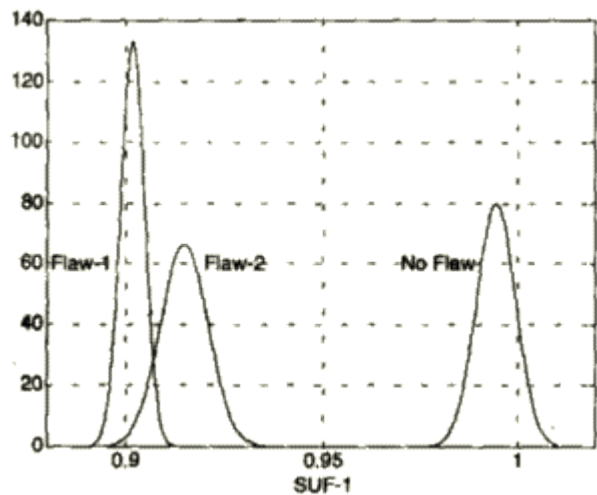
assembly line where couplant may be controlled, significant transducer couplant correlation can be statistically ensemble of parts for sorting

accepting/rejecting criteria in a piece-part assembly line environment.

Impurities in the incoming steel used to forge piece parts may result in sulfite stringer inclusions. In this next example simulated defects were created by placing a magnetized steel wire on the surface of a small steel cylindrical piston used in hydraulic transmissions.



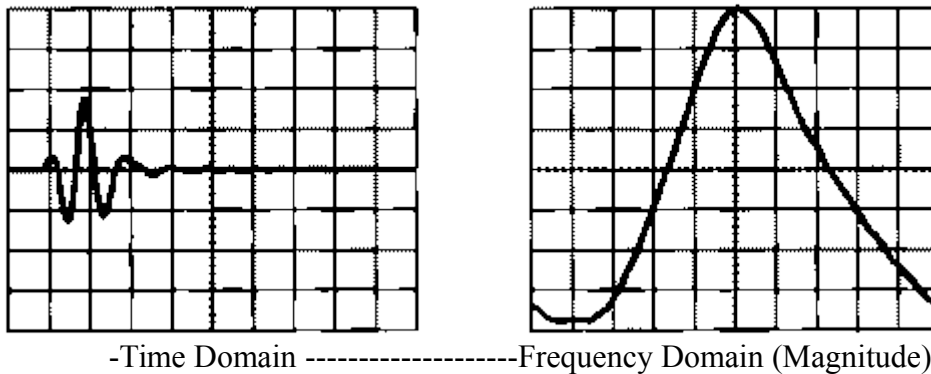
Two discrimination techniques are tested here, which are SUF-1 and SUF-2, with the latter giving the best discrimination between defect conditions. The important point being that spread spectrum ultrasonics can be extremely sensitive to the acoustic state of a part or structure being tested, and therefore, is a good ultrasonic candidate for testing and monitoring, especially where scanning is economic unfeasible.



## Signal Processing Techniques

Signal processing involves techniques that improve our understanding of information contained in received ultrasonic data. Normally, when a signal is measured with an oscilloscope, it is viewed in the time domain (vertical axis is amplitude or voltage and the horizontal axis is time). For many signals, this is the most logical and intuitive way to view them. Simple signal processing often involves the use of gates to isolate the signal of interest or frequency filters to smooth or reject unwanted frequencies.

When the frequency content of the signal is of interest, it makes sense to view the signal graph in the frequency domain. In the frequency domain, the vertical axis is still voltage but the horizontal axis is frequency.

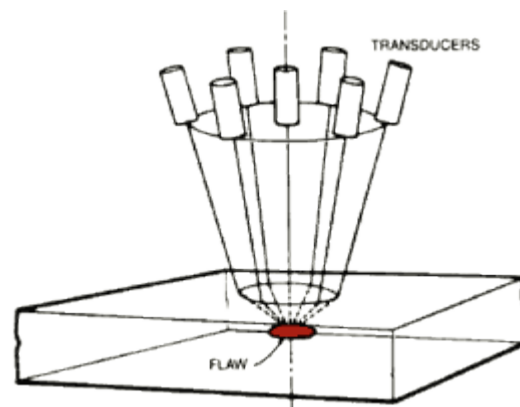


The frequency domain display shows how much of the signal's energy is present as a function of frequency. For a simple signal such as a sine wave, the frequency domain representation does not usually show us much additional information. However, with more complex signals, such as the response of a broad bandwidth transducer, the frequency domain gives a more useful view of the signal.

Fourier theory says that any complex periodic waveform can be decomposed into a set of sinusoids with different amplitudes, frequencies and phases. The process of doing this is called Fourier Analysis, and the result is a set of amplitudes, phases, and frequencies for each of the sinusoids that makes up the complex waveform. Adding these sinusoids together again will reproduce exactly the original waveform. A plot of the frequency or phase of a sinusoid against amplitude is called a spectrum.

## Flaw Reconstruction Techniques

In nondestructive evaluation of structural material defects, the size, shape, and orientation are important flaw parameters in structural integrity assessment. To illustrate flaw reconstruction, a multiviewing ultrasonic transducer system is shown below. A single probe moved sequentially to achieve different perspectives would work equally as well. The apparatus and the signal-processing algorithms



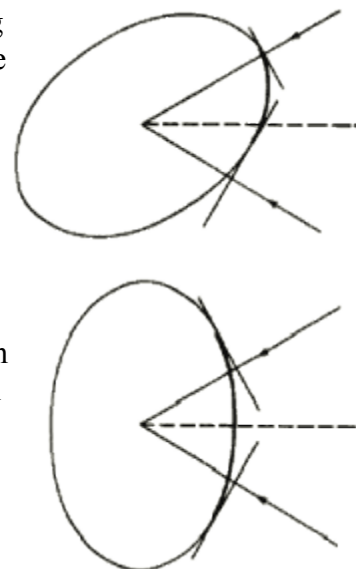
were specifically designed at the Center for Nondestructive Evaluation to make use of the theoretical developments in elastic wave scattering in the long and intermediate wavelength regime.

Depicted schematically at the right is the multiprobe system consisting of a sparse array of seven unfocused immersion transducers. This system can be used to "focus" onto a target flaw in a solid by refraction at the surface. The six perimeter transducers are equally spaced on a 5.08 cm diameter ring, surrounding a center transducer. Each of the six perimeter transducers may be independently moved along its axis to allow an equalization of the propagation time for any pitch-catch or pulse-echo combinations. The system currently uses 0.25 in diameter transducers with a nominal center frequency of 10 MHz and a bandwidth extending from approximately 2 to 16 MHz. The axis of the aperture cone of the transducer assembly normally remains vertical and perpendicular to the part surface.

The flaw reconstruction algorithm normally makes use of 13 or 19 backscatter waveforms acquired in a conical pattern within the aperture. The data-acquisition and signal-processing protocol has four basic steps.

1. Step one involves the experimental setup, the location and focusing on a target flaw, and acquisition (in a predetermined pattern) of pitch-catch and pulse-echo backscatter waveforms.
2. Step two employs a measurement model to correct the backscatter waveforms for effects of attenuation, diffraction, interface losses, and transducer characteristics, thus resulting in absolute scattering amplitudes.
3. Step three employs a one-dimensional **inverse Born approximation** to extract a tangent plane to centroid radius estimate for each of the scattering amplitudes.
4. In step four the radius estimates and their corresponding look angles are used in a regression analysis program to determine the six ellipsoidal parameters, three semi-axes, and three Euler angles, defining an ellipsoid which best fits the data.

The inverse Born approximation sizes the flaw by computing the characteristic function of the flaw (defined as unity inside the flaw and zero outside the flaw) as a Fourier transform of the ultrasonic scattering amplitude. The one-dimensional inverse Born algorithm treats scattering data in each interrogation direction independently and has been shown to yield the size of ellipsoidal flaws (both voids and inclusions) in terms of the distance from the center of the flaw to the wavefront that is tangent to the front surface of the flaw. Using the multiprobe ultrasonic system, the 1-D inverse Born technique is used to reconstruct voids and inclusions that can be reasonably approximated by an equivalent ellipsoid. So far, the investigation has been confined to convex flaws with a center of inversion symmetry. The angular scan method described in this paper is capable of locating the bisecting symmetry planes of a flaw. The utility of the multiprobe



system is, therefore, expanded since two-dimensional elliptic reconstruction may now be made for the central slice. Additionally, the multiprobe system is well suited for the 3-D flaw reconstruction technique using 2-D slices.

The model-based reconstruction method has been previously applied to voids and inclusion flaws in solids. Since the least-squares regression analysis leading to the "best fit" ellipsoid is based on the tangent plane to centroid distances for the interrogation directions confined within a finite aperture. The success of reconstruction depends on the extent of the flaw surface "illuminated" by the various viewing directions. The extent of coverage of the flaw surface by the tangent plane is a function of the aperture size, flaw shape, and the flaw orientation. For example, a prolate spheroidal flaw with a large aspect ratio oriented along the axis of the aperture cone will only have one tip illuminated (i.e., covered by the tangent planes) and afford a low reconstruction reliability. For the same reason, orientation of the flaw also has a strong effect on the reconstruction accuracy.

The diagram on the right shows the difference in surface coverage of a tilted flaw and an untilted flaw subjected to the same insonification aperture. Both the experimental and simulation studies of the aperture effect reported before were conducted for oblate and prolate spheroids oriented essentially symmetrically with respect to the part surface and hence the aperture cone. From a flaw reconstruction standpoint, an oblate spheroid with its axis of rotational symmetry perpendicular to the part surface represents a high leverage situation. Likewise, a prolate spheroid with its symmetry axis parallel to the part surface also affords an easier reconstruction than a tilted prolate spheroid. In this CNDE project, we studied effects of flaw orientation on the reconstruction and derived a new data-acquisition approach that will improve reliability of the new reconstruction of arbitrarily oriented flaws.

The orientation of a flaw affects reconstruction results in the following ways.

1. For a given finite aperture, a change in flaw orientation will change the insonified surface area and hence change the "leverage" for reconstruction.
2. The scattering signal amplitude and the signal/noise ratio for any given interrogation direction depends on the flaw orientation.
3. Interference effects, such as those due to tip diffraction phenomena or flash points may be present at certain orientations. Of course, interdependencies exist in these effects, but for the sake of convenience they are discussed separately in the following.

## **Aperture**

To assess the effects of finite aperture size on flaws of different orientation, computer simulations were performed for an oblate spheroid with semi-axes of 400, 400, and 200  $\mu\text{m}$  that is tilted and untilted with respect to the part surface. For each of the 13 scattering directions, the exact radius estimates  $R_e$  (i.e. the tangent plane to centroid distances) were first computed, and a random error in sizing was then introduced to simulate the experimental situation. The radius estimate used was then taken to be

$$R_e' = R_e (I + n)$$

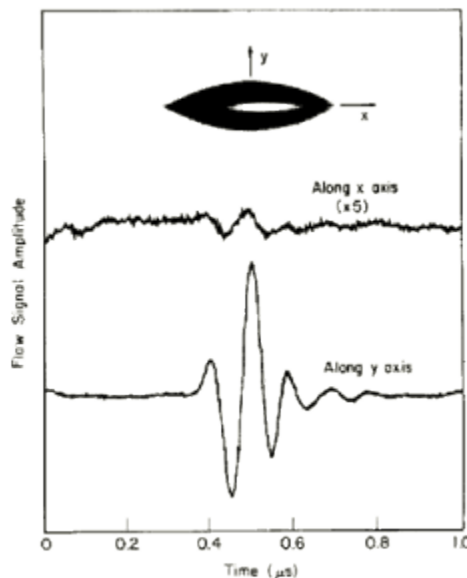
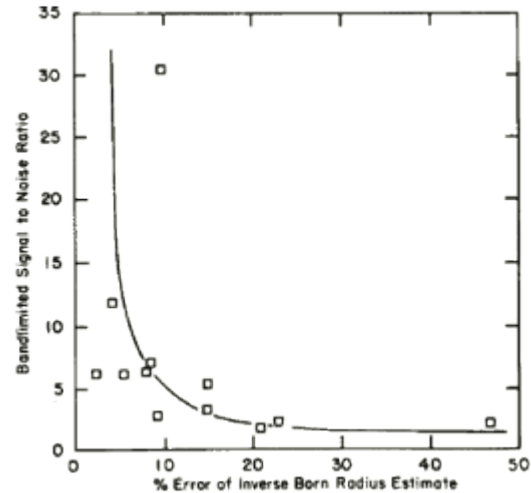
where  $n$  is a randomly generated number between  $\pm 0.1$ . Using the  $R_e'$  values for the various directions, a best fit ellipsoid is determined using a regression program. This process is repeated 100 times for each aperture angle and mean standard deviation of the three semi-axes is expressed as a percentage of the expected values. The simulation was performed for the untilted case with the  $400 \times 400 \mu\text{m}$  plane parallel to the part surface and for a tilt angle of  $40f$  from the normal of the part surface. The results are summarized in Table I.

TABLE I  
RECONSTRUCTION ERROR FOR A TILTED FLAW AND AN UNTILTED FLAW

Aperture Half-Angle ( ° )	Standard Deviation as a Percentage of the Expected Semi-Axes Value for the 2 : 1 Oblate Spheroid	
	Tilt = 0° (percent)	Tilt = 40° (percent)
20	11.6	39.0
30	6.9	18.2
40	4.5	10.9
50	4.3	7.6
60	4.1	5.8
70	4.1	4.6
80	4.1	4.0

The mean values for the ellipsoidal semi-axes converge to expected values, while the standard deviations converge to some asymptotic minimum. The values in Table I show that for a small aperture, the standard deviation as a percentage of expected value (an indication of the reconstruction error) is much higher for the oblate spheroid tilted at  $40f$  with respect to the horizontal than is the  $0f$  untilted case. As the aperture increases, the difference in reconstruction error approaches zero because surface illumination is sufficient to ensure a reliable reconstruction. Due to the combined effect of finite aperture and a prior unknown flaw orientation, a large aperture is desirable to increase reliability of reconstruction results.

Note that in this simulation only the aperture angle is increased, and the number of interrogation directions remains unchanged. The number of look directions is kept the same because the multiviewing system is intended for acquiring a sparse array of data based on speed considerations.



## Signal/Noise Ratio

For a given scattering direction amplitude of the scattering amplitude and, therefore, the signal/noise ratio depend on orientation of the flaw. In the short wavelength limit scattering amplitude is proportional to square root of  $(R_1 R_2)$  with  $R_1$  and  $R_2$  being the principal radii of curvature of the flaw for the scattering direction used. This dependence is found to be important in the intermediate frequency regime as well. To illustrate this effect, the figure at the right shows the scattered signal amplitudes from a football-shaped prolate spheroidal void with two cusp-like tips in two directions: broadside and along the tips. The profile of the tips can increase the ratio of the two signal amplitudes as large as 35.

To investigate the correlation between the accuracy of flaw sizing and signal/noise ratio of the flaw waveform at different scattering directions, a  $400 \times 400 \times 200 \mu\text{m}$  oblate spheroidal void in titanium with its axis of rotational symmetry tilted at a  $30f$  angle from normal to the part surface was reconstructed using the multiviewing transducer system. It was found that sizing results were generally more accurate for the scattering directions with a higher signal/noise ratio, as expected. Furthermore, the directions that gave the poorest signal/noise ratios were often ones closest to being in an edge-on perspective. The figure on the right shows the relationship between the percentage error of the radius estimate and signal/noise ratio of the flaw waveform. Reconstruction results of the oblate spheroid void tilted at  $30f$  are listed in Table II.

**TABLE II**  
RECONSTRUCTION RESULTS FOR A 2 : 1 OBLATE SPHEROID IN TITANIUM WITH  
A  $30^\circ$  TILT USING AN APERTURE OF  $52^\circ$  HALF-ANGLE\*

		Obtained from Full Set of 13 Backscatter Waveforms	Obtained from Best Nine Back- scatter Wave- forms Based on S/N Ratio	Expected Values
Ellipsoid semi- axis ( $\mu\text{m}$ )	$A_x$	456	400	400
	$A_y$	351	380	400
	$A_z$	177	184	200
Euler angles ( $^\circ$ )	$\theta$	-51	-36	30
	$\phi$	79	73	-90
	$\psi$	9	28	0

\*When comparing the flaw orientation in terms of Euler angles, the entire set of angles should be used. The flaw orientations in the last two columns are, in fact, quite close to being equivalent.

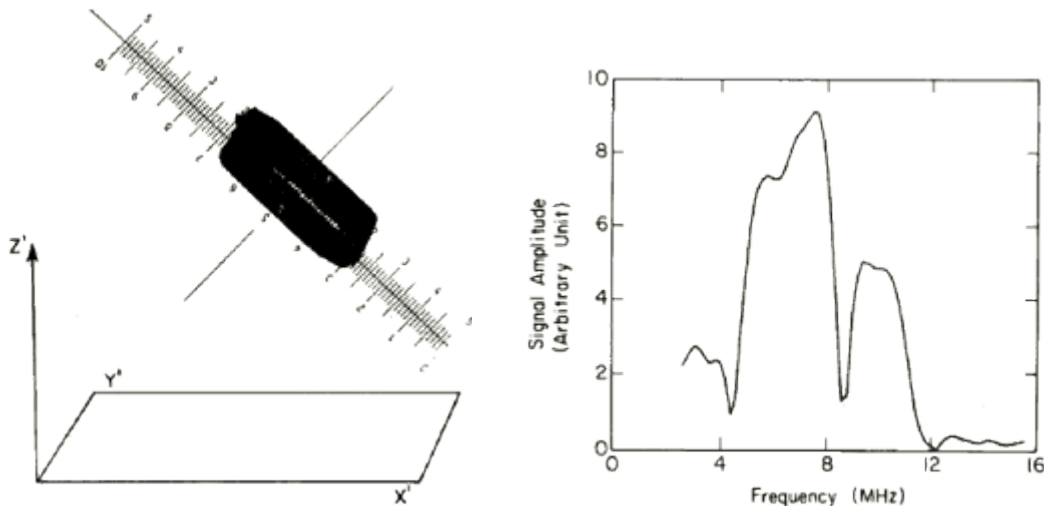
The reconstruction results of both the semi-axes length and tilt angle were improved by rejecting four data points with the lowest signal/noise ratios. Since multiviewing transducer system provides a maximum of 19 independent look angles for a given tilt angle of the transducers, rejecting a small subset of the data points based on signal/noise

consideration still leaves a sufficient number of data points for the ellipsoidal regression step which requires a minimum of six data points.

### Flash Point Interference

The multiview transducer system and associated signal-processing algorithms reconstruct a flaw based on a general ellipsoid model. For ellipsoids with a large aspect ratio and flaw shapes that approach those of a flat crack or a long needle, edge or tip diffractions due to points of stationary phase (flash points) governed by, geometric acoustics become important. When such phenomena are present within the transducer bandwidth, the scattered signal frequency spectrum contains strong interference maxima and minima and renders radius estimates by the 1-D inverse Born difficult or impossible.

The figures below show a test flaw in the form of a copper wire segment embedded in a transparent thermoplastic disk and tilted at  $45^\circ$  with respect to the disk surface and the frequency spectrum of the wire inclusion at a scattering angle of  $21^\circ$  from the wire axis. The strong interference pattern prevented the I-D inverse Born algorithm from yielding a meaningful radius estimate. However, when the spectrum was analyzed on assumption of flash point interference (without having to use the angle information),  $321 \mu\text{m}$  was obtained for a path length difference of the stationary phase points in the scattering direction; this compared reasonably well with  $374 \mu\text{m}$  for twice the tangent plane distance in this orientation.



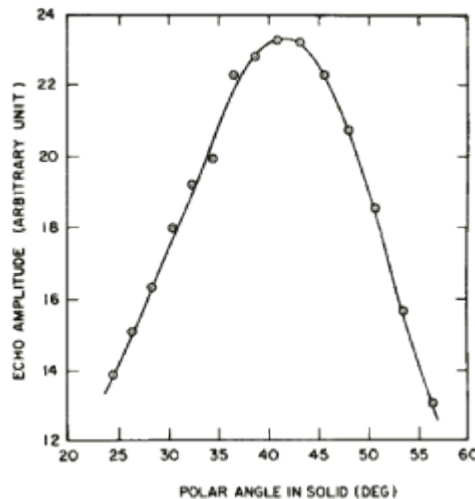
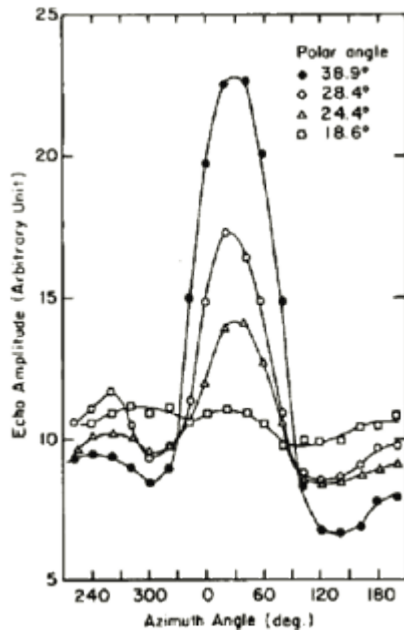
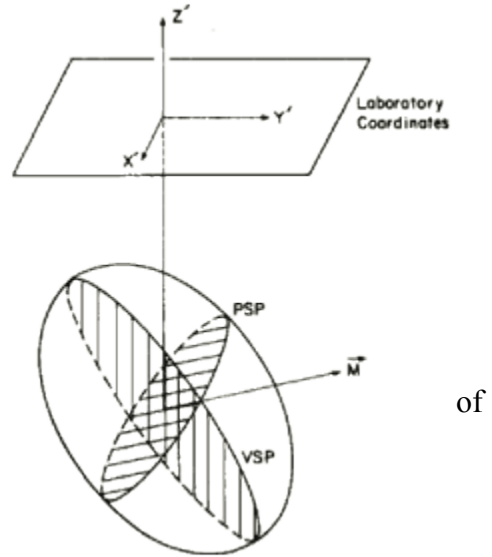
Photomicrograph of copper wire segment tilted at  $45^\circ$  and embedded in thermoplastic. Each minor division of scale is  $10 \mu\text{m}$ , and wire segment is approximately prolate spheroid with semi-axes  $A_x = 80 \mu\text{m}$ ,  $A_y = 80 \mu\text{m}$ , and  $A_z = 200 \mu\text{m}$ .

### Spatial Data-acquisition Pattern For Arbitrarily Oriented Flaw

From the investigation described earlier, it is clear that reliable reconstruction of an arbitrarily oriented flaw generally requires a large aperture. However, a large viewing aperture perpendicular to the part surface may still contain scattering directions hampered by weak flaw signal amplitude (poor signal-to-noise ratio) and, in certain cases, flash

point interference. A predetermined data-acquisition pattern that is relatively free from such disadvantages can improve reconstruction reliability. In this work we explored a method to predetermine a spatial pattern for data acquisition. This pattern affords a high leverage for reliable reconstruction for arbitrarily oriented flaws that can be approximated by the shape of a spheroid.

Consider a tilted prolate spheroid as shown on the right. We may define a vertical sagittal plane (VSP) as the plane that bisects the flaw and contains the  $z$  axis. We further define a perpendicular sagittal plane (PSP) as the plane bisecting the spheroid and perpendicular to the VSP. The intersection of the VSP and PSP (direction  $M$  in diagram) then corresponds to a direction of maximum flaw signal amplitude. The orientation of the VSP can be located by a series azimuthal scans at different polar angles. A maximum in the signal amplitude should be observed at the azimuthal angle of the VSP. This definition of the VSP and PSP and their relationship to backscattered flaw signal amplitude also holds true for an oblate spheroid. Below shows the azimuthal scans at four different polar angles for the 2.5:1 prolate spheroid (wire segment) flaw. Once the azimuthal angle of the VSP is determined ( $30^\circ$  in this case), a polar scan below at the azimuthal angle of the VSP determines the tilt angle of the wire segment to be  $41^\circ$ , as compared to  $45^\circ$  from optical measurement.



Flaw signal amplitude as a function of azimuthal and polar angles.

The angular scans serve two very useful functions. First, they provide some information about the shape and orientation of the flaw. For example, a scan in the perpendicular sagittal plane can distinguish a prolate spheroid from an oblate spheroid by changing the

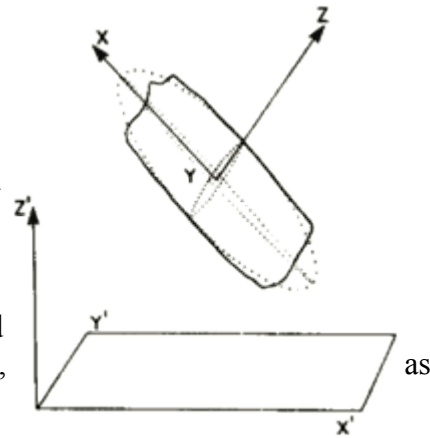
polar angle and the azimuthal angle simultaneously. A scan in the PSP of the 2:1 oblate spheroid tilted at  $30^\circ$  showed a peak in flaw signal amplitude at the intersection of the VSP and the PSP (direction M), whereas a scan in the PSP of the tilted 2.5:1 prolate spheroid showed a constant flaw signal amplitude.

Second, it provides a basis for predetermining a spatial data-acquisition pattern that is equivalent to a tilted aperture cone centered at direction M. This data-acquisition pattern not only ensures good signal-to-noise ratio, avoids possible flash point interference due to end-on or edge-on perspectives, and provides a maximum illuminated area on the flaw surface, but also allows one to reconstruct the flaw with two mutually orthogonal elliptical cross sections in the VSP and PSP.

So far, the discussion of angular scans has been confined to flaws that are approximately spheroidal in shape. For a general ellipsoid with three unequal semi-axes and oriented arbitrarily in space, the angular scan results will be more complicated. For example, an azimuthal scan at different polar angles is not expected to show a peak at the same azimuthal angle. Shape and orientation information, in principle, can still be extracted from such data, and further investigations are underway for the general case.

## Reconstruction Results

To verify the reconstruction method using the new spatial data-acquisition configuration experimentally, reconstructions were performed on two test specimens. The first flaw was the 400  $\mu\text{m}$  long 80  $\mu\text{m}$  radius copper wire segment embedded in a thermoplastic disk. This flaw was used to approximate a prolate spheroid with a 2.5:1 aspect ratio. The axis of the wire segment was at a  $45^\circ$  angle relative to the part surface. The second flaw was a 400 x 200  $\mu\text{m}$  oblate spheroidal void tilted at a  $30^\circ$  angle in a diffusion bonded titanium disk, just described.



The flaw reconstruction procedure using an aperture cone perpendicular to the part surface was first carried out for the 2.5:1 prolate inclusion (copper wire) tilted at a  $45^\circ$  angle. Difficulties due to a poor signal-to-noise ratio and flash point interference associated with look directions close to the end-on perspective prevented a successful reconstruction; in fact, enough inconsistencies occurred in the tangent plane distance estimates that the regression step failed to converge.

Based on orientations of the sagittal planes determined in the angular scans, the new data-acquisition pattern equivalent to tilting the aperture axis to the direction of maximum signal strength was used. The ellipsoidal reconstruction gave a tilt angle of  $42^\circ$  and three semi-axes of 257, 87, and 81  $\mu\text{m}$ . These results compared very favorably with the actual tilt angle of  $45^\circ$  and the actual semi-axes of 200, 80, and 80  $\mu\text{m}$ .

The new data-acquisition pattern also allows one to reconstruct an arbitrarily tilted spheroidal flaw with the two mutually orthogonal elliptical cross-sectional cuts in the

VSP and PSP. This was done for the copper wire inclusion. After identifying the vertical sagittal plane and the perpendicular sagittal plane, a series of tangent plane distance estimates were made for scattering directions confined in these two planes. Using these results, the two mutually orthogonal elliptical cross sections in the VSP and PSP were reconstructed using a similar regression program in 2-D. The two reconstructed ellipses were  $266 \times 83 \mu\text{m}$  and  $80 \times 75 \mu\text{m}$ , respectively, and the tilt angle was found to be  $51f$ . Table III shows the results of the 3-D reconstruction using 19 look perspectives and the 2-D reconstruction of the ellipses in the VSP and PSP. Both reconstructions compared very favorably with the expected values. The greatest discrepancy is in the value of the semi-axis  $A_x$ ; this is to be expected because the wire segment is approximately a prolate spheroid with two ends truncated.

TABLE III  
COPPER WIRE INCLUSION AS PROLATE SPHEROID

		3-D Reconstruction	2-D Reconstruction	Expected Values
Ellipsoid semi- axis ( $\mu\text{m}$ )	$A_x$	257	266	200
	$A_y$	87	80, 83	80
	$A_z$	81	75	80
Euler angles ( $^\circ$ )	$\theta$	42	51	45
	$\phi$	103	—	—
	$\psi$	74	—	—

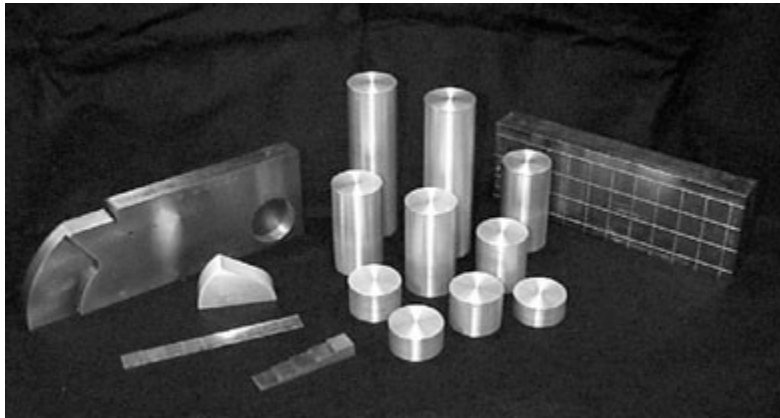
The 2:1 oblate spheroidal void tilted at a  $30f$  angle in a titanium disk was investigated, again, following the procedure of predetermining a favorable data-acquisition pattern based on angular scan results. Table IV shows the reconstruction results using the new data-acquisition pattern equivalent to an aperture cone centered on the direction of maximum backscatter signal. As a comparison, reconstruction results using an aperture cone normal to the part surface (described earlier) are also shown. As can be seen, the improvement of the reconstruction by using the new data-acquisition pattern is not as dramatic as the prolate inclusion case. This is consistent with the fact that the oblate spheroid has a smaller aspect ratio and a smaller tilt angle and is therefore not nearly a "low leverage" flaw to reconstruct using the normal (untilted) data-acquisition pattern.

TABLE IV  
RECONSTRUCTION RESULTS FOR A 2 : 1 OBLATE SPHEROID IN TITANIUM WITH  
A  $30^\circ$  TILT USING AN APERTURE OF  $52^\circ$

		Aperture Cone Normal to Part Surface (Based on Nine Look Directions)	Aperture Cone in the Direction of Maximum Backscatter Signal	Expected Values
Ellipsoid semi- axis ( $\mu\text{m}$ )	$A_x$	400	394	400
	$A_y$	380	419	400
	$A_z$	184	191	200
Euler angles ( $^\circ$ )	$\theta$	-36	31	30
	$\phi$	73	-89	-90
	$\psi$	28	3	0

The reliability problem of reconstructing arbitrarily oriented flaws using the multiviewing transducer system and associated model-based algorithm has been studied. An arbitrarily oriented flaw may afford a low leverage for reconstructing the entire flaw based on limited surface area covered by the tangent planes in a finite aperture and, therefore, requires a greater aperture for a reliable reconstruction. However, the aperture size has practical limits in a single-side access inspection situation and a larger aperture does not necessarily alleviate such difficulties as poor signal-to-noise ratio and flash point interference associated with certain interrogation directions.

## Calibration Methods



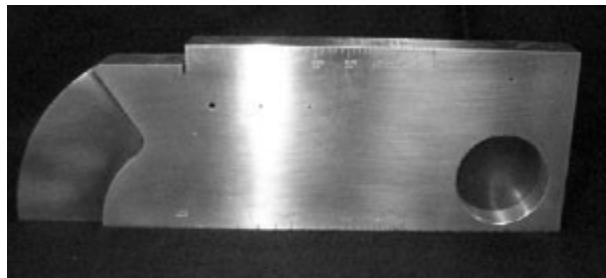
Calibration refers to the act of evaluating and adjusting the precision and accuracy of measurement equipment. In ultrasonic testing, several forms of calibration must occur. First, the electronics of the equipment must be calibrated to assure that they are performing as designed. This operation is usually performed by the equipment manufacturer and will not be discussed further in this material. It is also usually necessary for the operator to perform a "user calibration" of the equipment. This user calibration is necessary because most ultrasonic equipment can be reconfigured for use in a large variety of applications. The user must "calibrate" the system, which includes the equipment settings, the transducer, and the test setup, to validate that the desired level of precision and accuracy are achieved. The term calibration standard is usually only used when an absolute value is measured and in many cases, the standards are traceable back to standards at the National Institute for Standards and Technology.

In ultrasonic testing, there is also a need for reference standards. Reference standards are used to establish a general level of consistency in measurements and to help interpret and quantify the information contained in the received signal. Reference standards are used to validate that the equipment and the setup provide similar results from one day to the next and that similar results are produced by different systems. Reference standards also help the inspector to estimate the size of flaws. In a pulse-echo type setup, signal strength depends on both the size of the flaw and the distance between the flaw and the transducer. The inspector can use a reference standard with an artificially induced flaw of known size and at approximately the same distance away for the transducer to produce a signal. By comparing the signal from the reference standard to that received from the actual flaw, the inspector can estimate the flaw size. This section will discuss some of the more common calibration and reference specimen that are used in ultrasonic inspection. Some of these specimens are shown in the figure above. Be aware that there are other standards available and that specially designed standards may be required for many applications. The information provided here is intended to serve a general introduction to the standards and not to be instruction on the proper use of the standards.

### Introduction to the Common Standards

Calibration and reference standards for ultrasonic testing come in many shapes and sizes. The type of standard used is dependent on the NDE application and the form and shape of the object being evaluated. The material of the reference standard should be the same as the material being inspected and the artificially induced flaw should closely resemble that of the actual flaw. This second requirement is a major limitation of most standard reference samples. Most use drilled holes and notches that do not closely represent real flaws. In most cases the artificially induced defects in reference standards are better reflectors of sound energy (due to their flatter and smoother surfaces) and produce indications that are larger than those that a similar sized flaw would produce. Producing more "realistic" defects is cost prohibitive in most cases and, therefore, the inspector can only make an estimate of the flaw size. Computer programs that allow the inspector to create computer simulated models of the part and flaw may one day lessen this limitation.

### **The IIW Type Calibration Block**

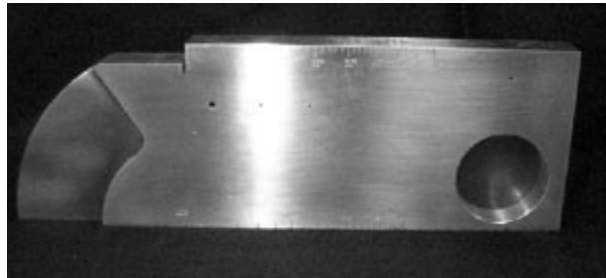


The standard shown in the above figure is commonly known in the US as an IIW type reference block. IIW is an acronym for the International Institute of Welding. It is referred to as an IIW "type" reference block because it was patterned after the "true" IIW block but does not conform to IIW requirements in IIS/IIW-23-59. "True" IIW blocks are only made out of steel (to be precise, killed, open hearth or electric furnace, low-carbon steel in the normalized condition with a grain size of McQuaid-Ehn #8) where IIW "type" blocks can be commercially obtained in a selection of materials. The dimensions of "true" IIW blocks are in metric units while IIW "type" blocks usually have English units. IIW "type" blocks may also include additional calibration and references features such as notches, circular groves, and scales that are not specified by IIW. There are two full-sized and a mini versions of the IIW type blocks. The Mini version is about one-half the size of the full-sized block and weighs only about one-fourth as much. The IIW type US-1 block was derived the basic "true" IIW block and is shown below in the figure on the left. The IIW type US-2 block was developed for US Air Force application and is shown below in the center. The Mini version is shown on the right.

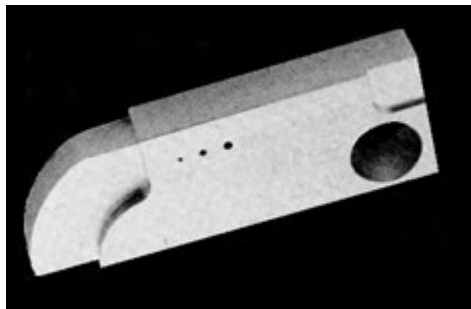
### **IIW Type US-1**



**IIW Type US-2**

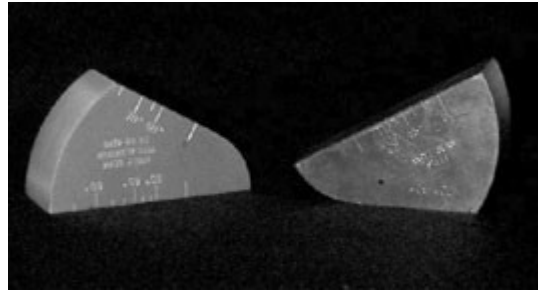


**IIW Type Mini**



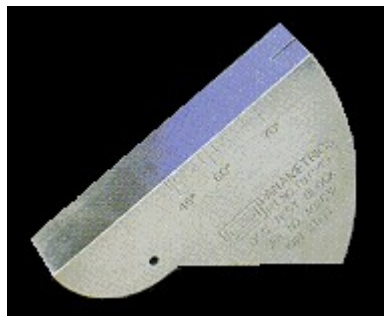
IIW type blocks are used to calibrate instruments for both angle beam and normal incident inspections. Some of their uses include setting metal-distance and sensitivity settings, determining the sound exit point and refracted angle of angle beam transducers, and evaluating depth resolution of normal beam inspection setups. Instructions on using the IIW type blocks can be found in the annex of American Society for Testing and Materials Standard E164, Standard Practice for Ultrasonic Contact Examination of Weldments.

### **The Miniature Angle-Beam or ROMPAS Calibration Block**



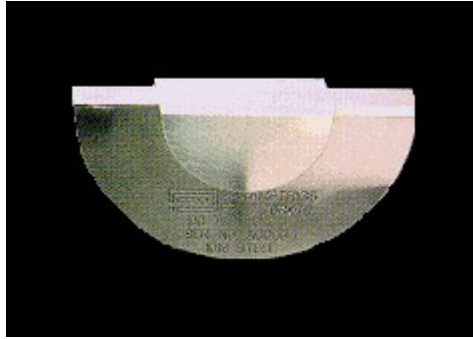
The miniature angle-beam is a calibration block that was designed for the US Air Force for use in the field for instrument calibration. The block is much smaller and lighter than the IIW block but performs many of the same functions. The miniature angle-beam block can be used to check the beam angle and exit point of the transducer. The block can also be used to make metal-distance and sensitivity calibrations for both angle and normal-beam inspection setups.

### **AWS Shearwave Distance/Sensitivity Calibration (DSC) Block**



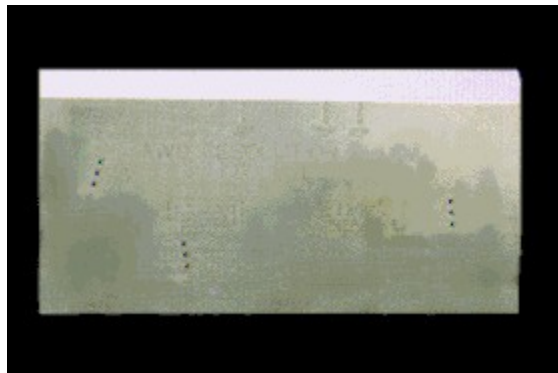
A block that closely resembles the miniature angle-beam block and is used in a similar way is the DSC AWS Block. This block is used to determine the beam exit point and refracted angle of angle-beam transducers and to calibrate distance and set the sensitivity for both normal and angle beam inspection setups. Instructions on using the DSC block can be found in the annex of American Society for Testing and Materials Standard E164, Standard Practice for Ultrasonic Contact Examination of Weldments.

### **AWS Shearwave Distance Calibration (DC) Block**



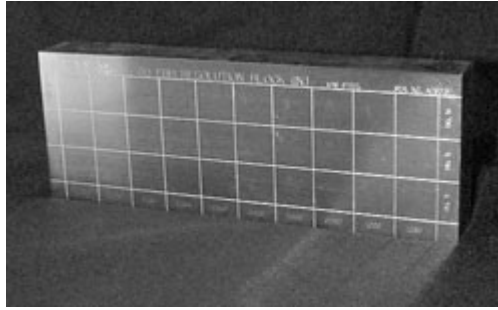
The DC AWS Block is a metal path distance and beam exit point calibration standard that conforms to the requirements of the American Welding Society (AWS) and the American Association of State Highway and Transportation Officials (AASHTO). Instructions on using the DC block can be found in the annex of American Society for Testing and Materials Standard E164, Standard Practice for Ultrasonic Contact Examination of Weldments.

### **AWS Resolution Calibration (RC) Block**



The RC Block is used to determine the resolution of angle beam transducers per the requirements of AWS and AASHTO. Engraved Index markers are provided for 45, 60, and 70 degree refracted angle beams.

### **30 FBH Resolution Reference Block**



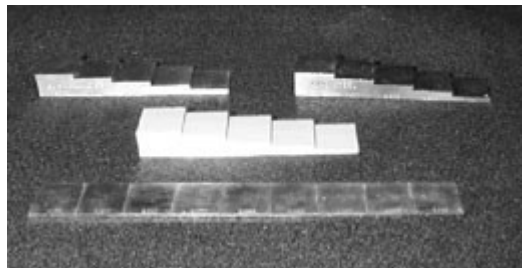
The 30 FBH resolution reference block is used to evaluate the near-surface resolution and flaw size/depth sensitivity of a normal-beam setup. The block contains number 3 (3/64"), 5 (5/64"), and 8 (8/64") ASTM flat bottom holes at ten metal-distances ranging from 0.050 inch (1.27 mm) to 1.250 inch (31.75 mm).

### **Miniature Resolution Block**



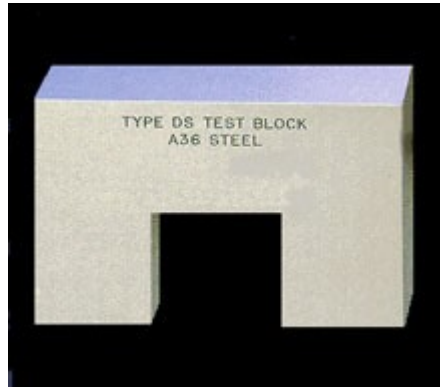
The miniature resolution block is used to evaluate the near-surface resolution and sensitivity of a normal-beam setup. It can be used to calibrate high-resolution thickness gages over the range of 0.015 inches (0.381 mm) to 0.125 inches (3.175 mm).

### **Step and Tapered Calibration Wedges**



Step and tapered calibration wedges come in a large variety of sizes and configurations. Step wedges are typically manufactured with four or five steps but custom wedge can be obtained with any number of steps. Tapered wedges have a constant taper over the desired thickness range.

### **Distance/Sensitivity (DS) Block**



The DS test block is a calibration standard used to check the horizontal linearity and the dB accuracy per requirements of AWS and AASHTO.

### **Distance/Area-Amplitude Blocks**



Distance/area amplitude correction blocks typically are purchased as a ten-block set, as shown above. Aluminum sets are manufactured per the requirements of ASTM E127 and steel sets per ASTM E428. Sets can also be purchased in titanium. Each block contains a single flat-bottomed, plugged hole. The hole sizes and metal path distances are as follows:

- 3/64" at 3"
- 5/64" at 1/8", 1/4", 1/2", 3/4", 1 1/2", 3", and 6"
- 8/64" at 3" and 6"

Sets are commonly sold in 4340 Vacuum melt Steel, 7075-T6 Aluminum, and Type 304 Corrosion Resistant Steel. Aluminum blocks are fabricated per the requirements of ASTM E127, Standard Practice for Fabricating and Checking Aluminum Alloy Ultrasonic Standard Reference Blocks. Steel blocks are fabricated per the requirements of ASTM E428, Standard Practice for Fabrication and Control of Steel Reference Blocks Used in Ultrasonic Inspection.

### **Area-Amplitude Blocks**

Area-amplitude blocks are also usually purchased in an eight-block set and look very similar to Distance/Area-Amplitude Blocks. However, area-amplitude blocks have a constant 3-inch metal path distance and the hole sizes are varied from 1/64" to 8/64" in 1/64" steps. The blocks are used to determine the relationship between flaw size and signal amplitude by comparing signal responses for the different sized holes. Sets are commonly sold in 4340 Vacuum melt Steel, 7075-T6 Aluminum, and Type 304 Corrosion Resistant Steel. Aluminum blocks are fabricated per the requirements of ASTM E127, Standard Practice for Fabricating and Checking Aluminum Alloy Ultrasonic Standard Reference Blocks. Steel blocks are fabricated per the requirements of ASTM E428, Standard Practice for Fabrication and Control of Steel Reference Blocks Used in Ultrasonic Inspection.

### **Distance-Amplitude #3, #5, #8 FBH Blocks**

Distance-amplitude blocks also very similar to the distance/area-amplitude blocks pictured above. Nineteen block sets with flat-bottom holes of a single size and varying metal path distances are also commercially available. Sets have either a #3 (3/64") FBH, a #5 (5/64") FBH, or a #8 (8/64") FBH. The metal path distances are 1/16", 1/8", 1/4", 3/8", 1/2", 5/8", 3/4", 7/8", 1", 1-1/4", 1-3/4", 2-1/4", 2-3/4", 3-1/4", 3-3/4", 4-1/4", 4-3/4", 5-1/4", and 5-3/4". The relationship between the metal path distance and the signal amplitude is determined by comparing signals from same size flaws at different depth. Sets are commonly sold in 4340 Vacuum melt Steel, 7075-T6 Aluminum, and Type 304 Corrosion Resistant Steel. Aluminum blocks are fabricated per the requirements of ASTM E127, Standard Practice for Fabricating and Checking Aluminum Alloy Ultrasonic Standard Reference Blocks. Steel blocks are fabricated per the requirements of ASTM E428, Standard Practice for Fabrication and Control of Steel Reference Blocks Used in Ultrasonic Inspection.

## **Distance Amplitude Correction (DAC)**

Acoustic signals from the same reflecting surface will have different amplitudes at different distances in the same material. A distance amplitude correction curve (DACC) can be constructed from the peak amplitude responses from reflectors of equal area at different distances in the same material.

Such curves are plotted specifically for a flat-bottom hole target and engraved on a transparent plastic sheet for attachment to the CRT screen. Disk-shaped reflectors, side drilled holes and hemispherical bottom holes are used as equivalent reflectors when using contact probes. A small steel ball helps to measure a distance-amplitude curve for immersion probes. These techniques are important because the amplitude of ultrasonic pulses varies with the distance from the probe, which causes the echo from a constant reflector to vary with distance. Therefore, to evaluate echoes of reflectors for all kind of probes, distance-amplitude curves are needed.

## **Curvature Corrections**

Planar contact ultrasonic transducers are commonly used to inspect components with curved surfaces. Examples include inspections of large diameter forgings, such as those used in electrical power generation equipment and in railroad rail. Previous work by Ying and Baudry (ASME 62-WA175, 1962) and by Birchak and Serabian (Mat. Eval. 36(1), 1978) derived methods for determining "correction factors" to account for degradation of signal amplitude as a function of the radius of curvature of convex, cylindrical components. Those methods were for narrowband (single frequency) inspections.

An alternative model for contact and immersion probe inspection now exists that models the liquid-solid in a manner similar to that employed by Ying and Baudry and by Birchak and Serabian. This model further predicts transducer radiation patterns using the Gauss-Hermite model, which has been used extensively for simulation of immersion mode inspections. The resulting model allows computationally efficient prediction of the full ultrasonic fields in the component for

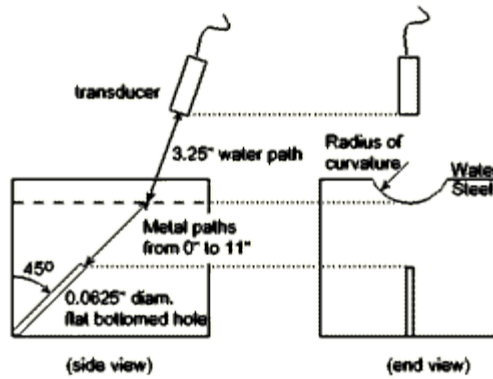
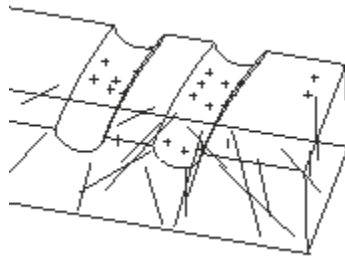
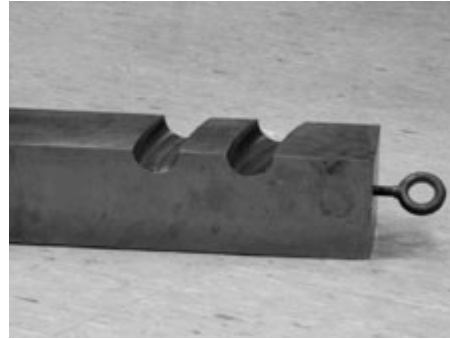
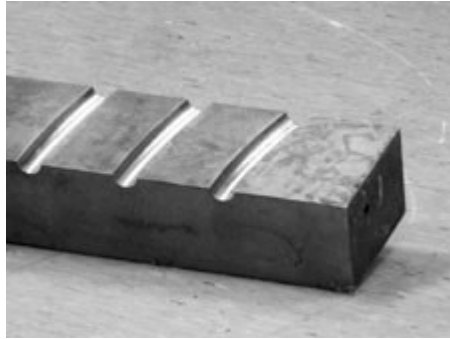
1. any frequency, including broadband measurements.
2. both circular and rectangular crystal shapes.
3. general component surface curvature
4. both normal and oblique incidence (e.g., angle beam wedges) transducers.

When coupled with analytical models for defect scattering amplitudes, the model can be used to predict actual flaw waveforms.

Example: Curvature Correction Factor Calculations #4 Flat Bottom Hole

The "correction" value is the change in amplitude needed to bring signals from a curved surface measurement to the DAC, or flat surface value. A 3.25" water path is assumed. The plotted data shows the DAC curve and a radius correction factor. The DAC curve

drops monotonically since a 3.25" water path ensures that the near field is in the water. The correction factor starts out negative because of the focusing effect of the curved surface. At greater depths, the correction factor is positive because of the increased beam spread beyond the focal zone caused by the surface curvature.

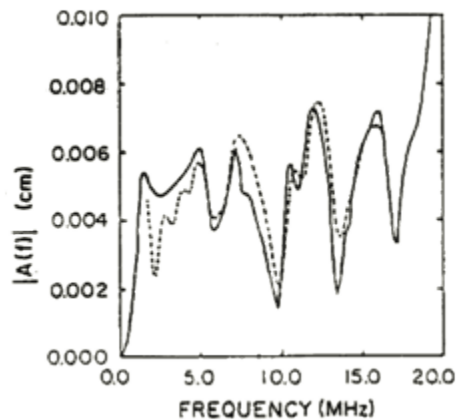


## Thompson-Gray Measurement Model

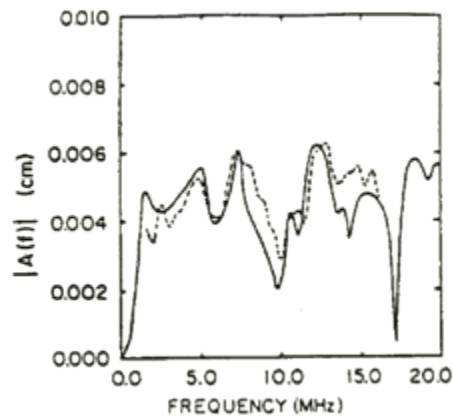
The Thompson-Gray Measurement Model allows the approximate prediction of ultrasonic scattering measurements made through liquid-solid interfaces. Liquid-solid interfaces are common in physical inspection scenarios. The model allows us to make predictions about received ultrasonic signals scattered from various classes of defects. The model predicts an absolute scattering amplitude in the sense that amplitudes are correct and transducer and system characteristics are removed by deconvolution techniques.

Work begun in the early 1980's continues to be refined and has resulted into an increasingly valuable working tool for comparison of ultrasonic theory and experiment. The Thompson-Gray Measurement Model is at the heart of UTSIM (see section 5.4 Ultrasonic Simulation - UTSIM).

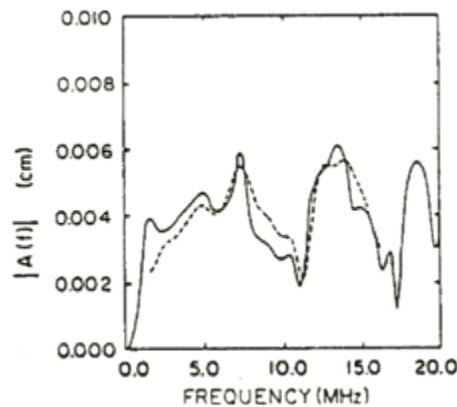
The validity of any model rests on how well its predictions agree with experiment. Shown below are three examples taken from the *J. Acoust. Soc. Am.*, 74(4) October 1983 entitled, "A model relating ultrasonic scattering measurements through liquid-solid interfaces to unbounded medium scattering amplitudes."



Comparison of theory and experimental magnitude of longitudinal pitch-catch scattering amplitude for a 114  $\mu\text{m}$  radius tin-lead solder sphere in a Lucite cylindrical disk. Illumination was at normal incidence and reception at an  $8^\circ$  angle ( $15^\circ$  in the solid).

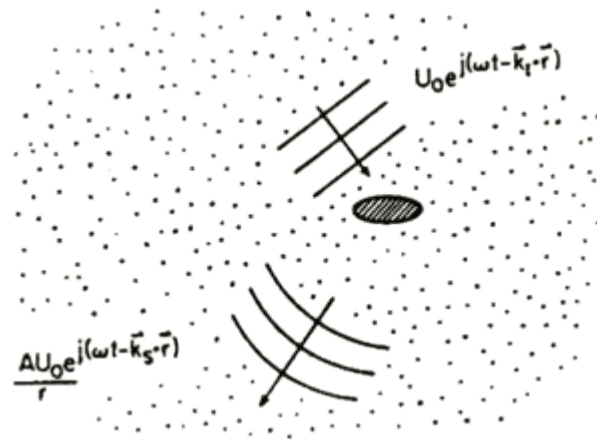


Comparison of theory and experimental magnitude of longitudinal pitch-catch scattering amplitude for a 114  $\mu\text{m}$  radius tin-lead solder sphere in a Lucite cylindrical disk. Illumination was at normal incidence and reception at an  $15.7^\circ$  angle ( $30^\circ$  in the solid).



Comparison of theory and experimental magnitude of longitudinal pitch-catch scattering amplitude for a 114  $\mu\text{m}$  radius tin-lead solder sphere in a Lucite cylindrical disk. Illumination was at normal incidence and reception at a  $22.5^\circ$  angle ( $45^\circ$  in the solid).

The relationship between scattering data obtained from ultrasonic experiments, in which the waves are excited and detected in a finite measurement geometry, and unbounded medium, farfield scattering amplitudes forms the basis of an ultrasonic measurement model.



Geometry of theoretical scattering calculation

For a scatterer in a single fluid medium, a Green's function approach is used to develop an approximate but absolute relationship between these experimental and theoretical cases.

Electromechanical reciprocity relationships are then employed to generalize to a two medium case in which the scatterer is located in an elastic solid which, along with the ultrasonic transducer, is immersed in a fluid medium.

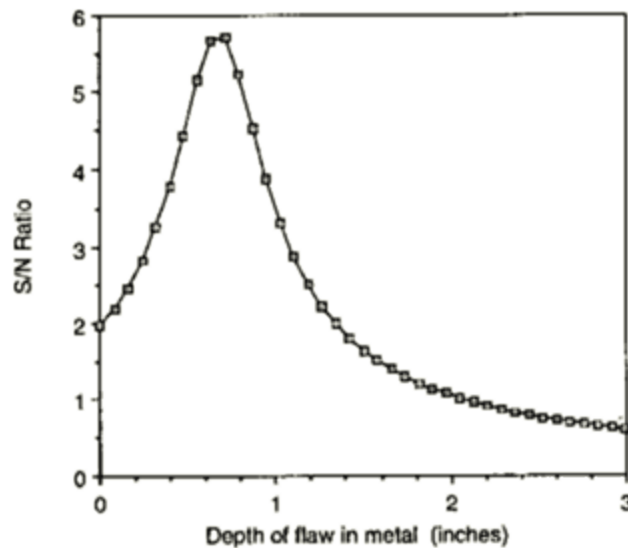
The scattering of elastic waves by a flaw in, an unbounded solid, e.g., a crack, void, or inclusion, is often characterized by a scattering amplitude  $A$  which defines the spherically spreading wave scattered into the farfield when the flaw is "illuminated" by a unit amplitude plane wave, as schematically illustrated in the above diagram. However, measurements of scattering are always made with transducers of finite aperture, at finite distances from the scatterer. Furthermore, the transducer is often immersed in a fluid medium and the wave has passed through the liquid-solid interface twice during the measurement. In principle, complete theoretical scattering solutions can be developed for this more complex scattering situation. However, even the introduction of the liquid-solid interface significantly complicates the elastic wave scattering and further introduction of finite beam effects in an exact manner would generally lead to computational complexity, which would severely restrict the use of the results in the routine interpretation of experiments. An alternative point of view would be to view the unbounded medium scattering amplitude  $A$  as a canonical solution and to develop approximate expressions, which relate this to the solutions for the more complex measurement geometries. This point of view is routinely adopted in studies of the acoustic scattering (e.g. sonar) from various obstacles. In that case, the problem is greatly simplified by (a) the fluid medium only supports a single wave type, (b) the waves do not pass through a refracting and mode converting interface, and (c) calibration experiments can be performed with arbitrary relative positions of transducers and reflecting surfaces to eliminate diffraction effects.

Included below is the derivation of an absolute measurement model relating the observed signals to scattering amplitudes for the case of small flaws.

## Grain Noise Modeling

In recent years, a number of theoretical models have been developed at Iowa State University to predict the electrical voltage signals seen during ultrasonic inspections of metal components. For example, the Thompson-Gray measurement model can predict the absolute voltage of the echo from a small defect, given information about the host metal (information such as density, sound speeds, surface curvature, etc.), the defect (size, shape, location, etc.), and the inspection system (water path, transducer characteristics, reference echo from a calibration block, etc.). If an additional metal property which characterizes the inherent noisiness of the metal microstructure is known, the independent scatterer model can be used to predict the absolute root-mean-squared (rms) level of the ultrasonic grain noise seen during an inspection. By combining the two models, [signal-to-noise](#) (S/N) ratios can be calculated.

Accurate model calculations often require intensive computer calculations. However, by making a number of approximations in the formalism, it is possible to obtain rapid first-order estimates of noise levels and S/N ratios. Our simplifying approximations are described in *Estimating Ultrasonic Signal-to-Noise Ratios for Inspections of Cylindrical Billets*. A FORTRAN computer program based on these approximations, SNCALC1, has been written, as well as a set of notes describing its use can be found *User Notes for SNCALC1: Software for Rapid Estimates of RMS Noise Levels and Signal-to-Noise Ratios*. Normal-incidence pulse-echo inspections through flat or curved surfaces are considered, and the flaw may be a flat crack or a spherical inclusion. The attached figures show the main menu and the results of one of the calculations described in the user notes. Calculations typically require only a few seconds on a PC.



## References & Standards

### What are standards?

Standards are documented agreements containing technical specifications or other precise criteria to be used consistently as rules, guidelines, or definitions of characteristics, in order to ensure that materials, products, processes, and services are fit for their purpose.

For example, the format of the credit cards, phone cards, and "smart" cards that have become commonplace is derived from an ISO International Standard. Adhering to the standard, which defines such features as an optimal thickness (0.76 mm), means that the cards can be used worldwide.

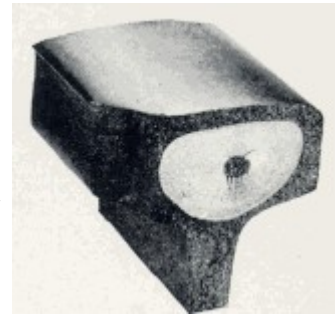
An important source of practice codes, standards, and recommendations for NDT is given in the *Annual Book of the American Society of Testing and Materials, ASTM*. The *Volume 03.03 Nondestructive Testing* is revised annually, covering acoustic emission, eddy current, leak testing, liquid penetrants, magnetic particle, radiography, thermography, and ultrasonics.

There are many efforts on the part of the National Institute of Standards and Technology (NIST) and other standards organizations, both national and international, to work through technical issues and harmonize national and international standards.

## Rail Inspection

One of the major problems that railroads have faced since the earliest days is the prevention of service failures in track. As is the case with all modes of high-speed travel, failures of an essential component can have serious consequences. The North American railroads have been inspecting their most costly infrastructure asset, the rail, since the late 1920's. With increased traffic at higher speed, and with heavier axle loads in the 1990's, rail inspection is more important today than it has ever been.

Although the focus of the inspection seems like a fairly well-defined piece of steel, the testing variables present are significant and make the inspection process challenging.

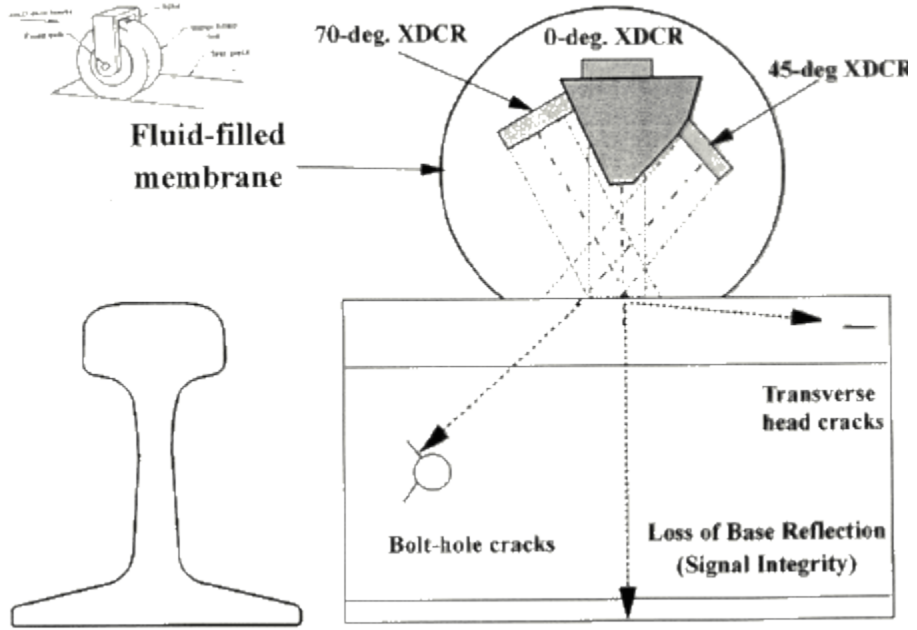


Rail inspections were initially performed solely by visual means. Of course, visual inspections will only detect external defects and sometimes the subtle signs of large internal problems. The need for a better inspection method became a high priority because of a derailment at Manchester, NY in 1911, in which 29 people were killed and 60 were seriously injured. In the U.S. Bureau of Safety's (now the National Transportation Safety Board) investigation of the accident, a broken rail was determined to be the cause of the derailment. The bureau established that the rail failure was caused by a defect that was entirely internal and probably could not have been detected by visual means. The defect was called a transverse fissure (example shown on the left). The railroads began investigating the prevalence of this defect and found transverse fissures were widespread.

One of the methods used to inspect rail is ultrasonic inspection. Both normal- and angle-beam techniques are used, as are both pulse-echo and pitch-catch techniques. The different transducer arrangements offer different inspection capabilities. Manual contact testing is done to evaluate small sections of rail but the ultrasonic inspection has been automated to allow inspection of large amounts of rail.

Fluid filled wheels or sleds are often used to couple the transducers to the rail. Sperry Rail Services, which is one of the companies that perform rail inspection, uses Roller Search Units (RSU's) comprising a combination of different transducer angles to achieve the best inspection possible. A schematic of an RSU is shown below.

# Wheel Probe Used in Railroad Rail Inspection

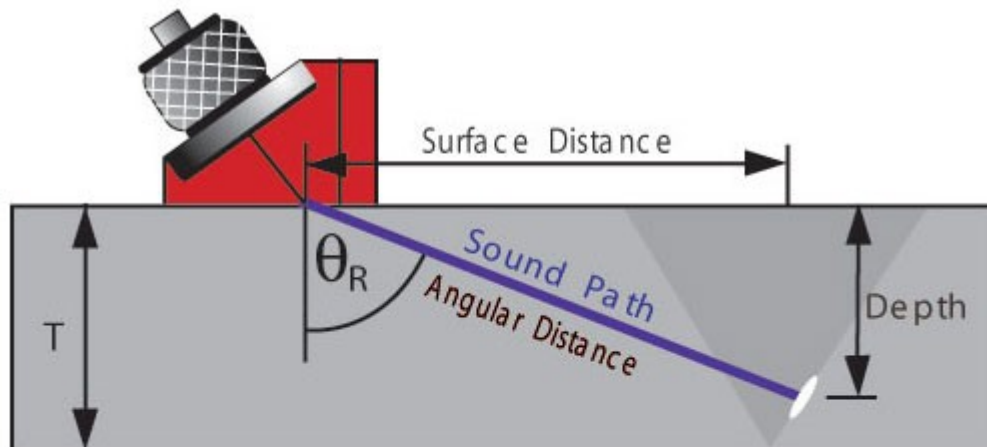


## Weldments (Welded Joints)

The most commonly occurring defects in welded joints are porosity, slag inclusions, lack of side-wall fusion, lack of inter-run fusion, lack of root penetration, undercutting, and longitudinal or transverse cracks.

With the exception of single gas pores all the defects listed are usually well detectable by ultrasonics. Most applications are on low-alloy construction quality steels, however, welds in aluminum can also be tested. Ultrasonic flaw detection has long been the preferred method for nondestructive testing in welding applications. This safe, accurate, and simple technique has pushed ultrasonics to the forefront of inspection technology.

Ultrasonic weld inspections are typically performed using a straight beam transducer in conjunction with an angle beam transducer and wedge. A straight beam transducer, producing a longitudinal wave at normal incidence into the test piece, is first used to locate any laminations in or near the heat-affected zone. This is important because an angle beam transducer may not be able to provide a return signal from a laminar flaw.



$\theta_R$  = Angle of Refraction

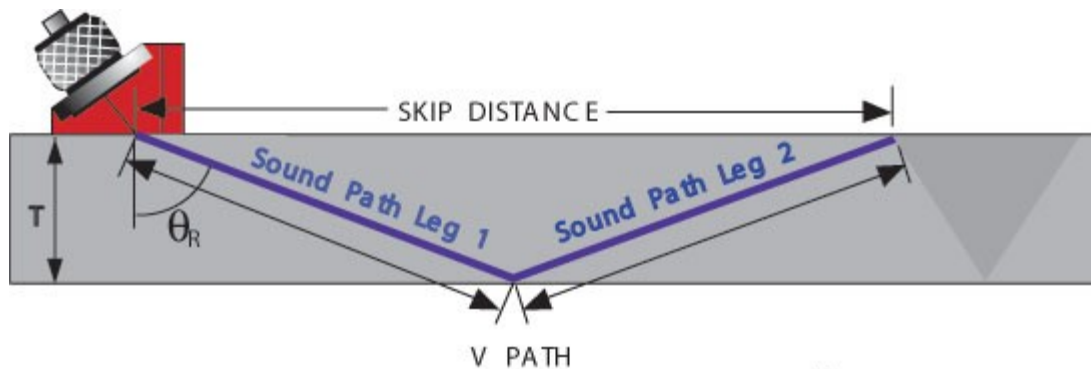
$T$  = Material Thickness

Surface Distance =  $\sin\theta_R \times$  Sound Path

Depth (1<sup>st</sup> Leg) =  $\cos\theta_R \times$  Sound Path

The second step in the inspection involves using an angle beam transducer to inspect the actual weld. Angle beam transducers use the principles of refraction and mode conversion to produce refracted shear or longitudinal waves in the test material. [Note: Many AWS inspections are performed using refracted shear waves. However, material having a large grain structure, such as stainless steel may require refracted longitudinal waves for successful inspections.] This inspection may include the root, sidewall, crown, and heat-

affected zones of a weld. The process involves scanning the surface of the material around the weldment with the transducer. This refracted sound wave will bounce off a reflector (discontinuity) in the path of the sound beam. With proper angle beam techniques, echoes returned from the weld zone may allow the operator to determine the location and type of discontinuity.



$\theta_R$  = Refracted Angle

$T$  = Material Thickness

Skip Distance =  $2T \times \tan\theta_R$

$$\text{Leg} = \frac{T}{\cos\theta_R}$$

$$\text{V-Path} = \frac{2T}{\cos\theta_R}$$

To determine the proper scanning area for the weld, the inspector must first calculate the location of the sound beam in the test material. Using the refracted angle, beam index point and material thickness, the V-path and skip distance of the sound beam is found. Once they have been calculated, the inspector can identify the transducer locations on the surface of the material corresponding to the crown, sidewall, and root of the weld.

